

A theoretical investigation for the role of electron-hole separation distance within metal-free 1,3,4-oxadiazoles dyes in the efficiencies of dye sensitized solar cells

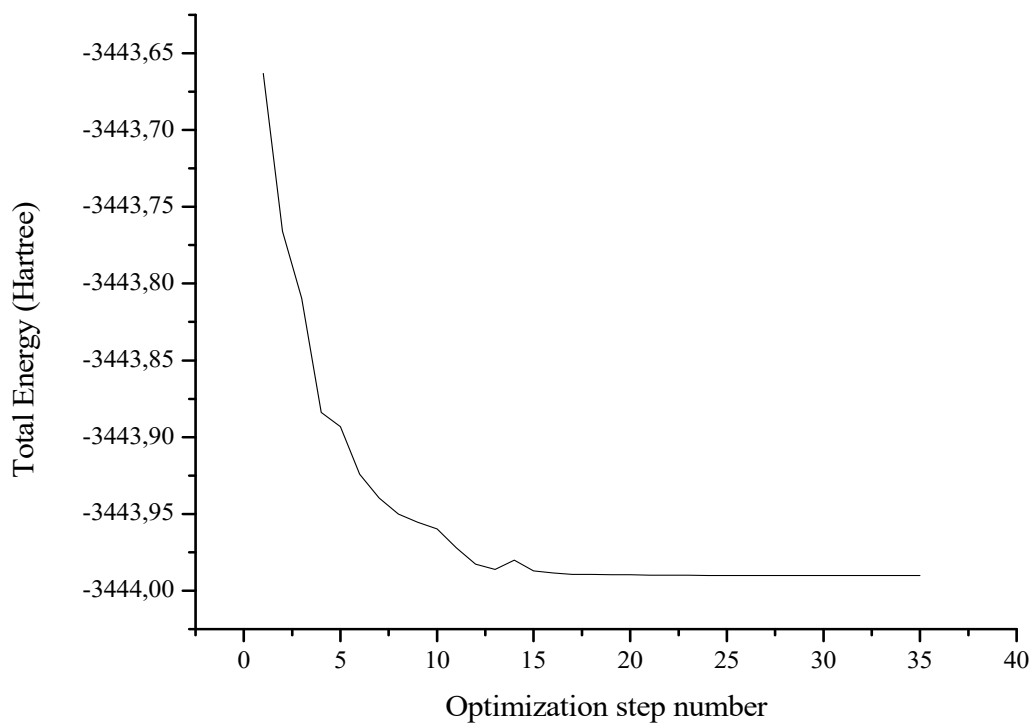
Louis-Charl Coetzee^a, Adedapo Adeyinka^a, Nomampondo Magwa^b,

^a*Chemical Sciences, University of Johannesburg, PO Box 524, Auckland Park, Johannesburg, 2006, Gauteng, South Africa.*

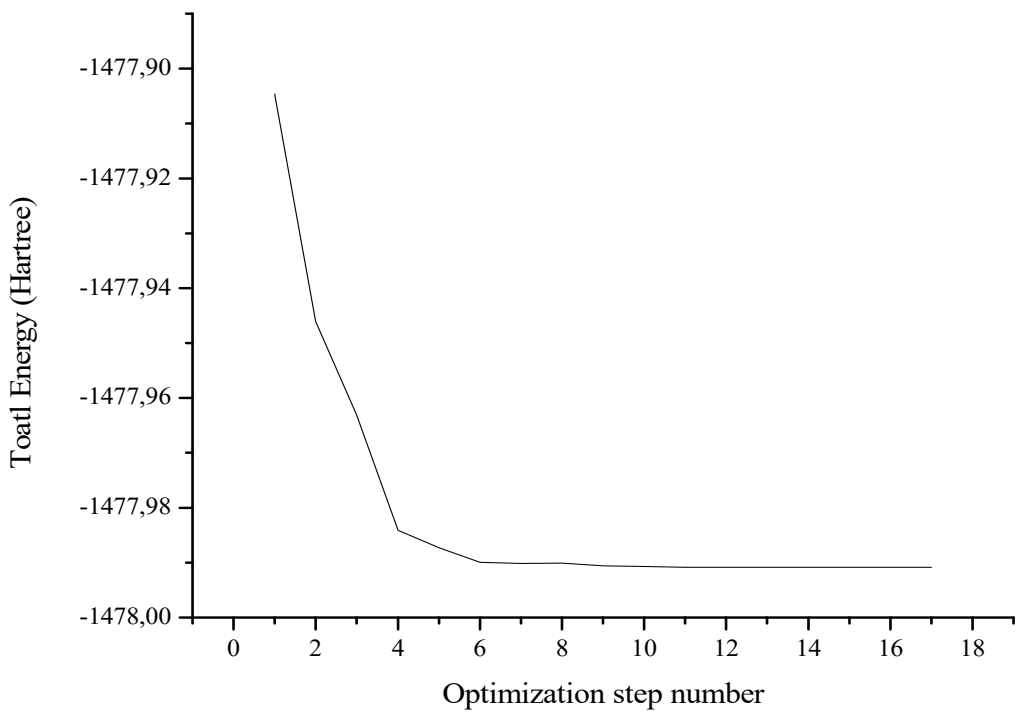
Tel.: +27604699790

^b*Department of Chemistry, University of South Africa, Private Bag X6, Florida, Roodepoort, Johannesburg, 1710, Gauteng, South Africa.*

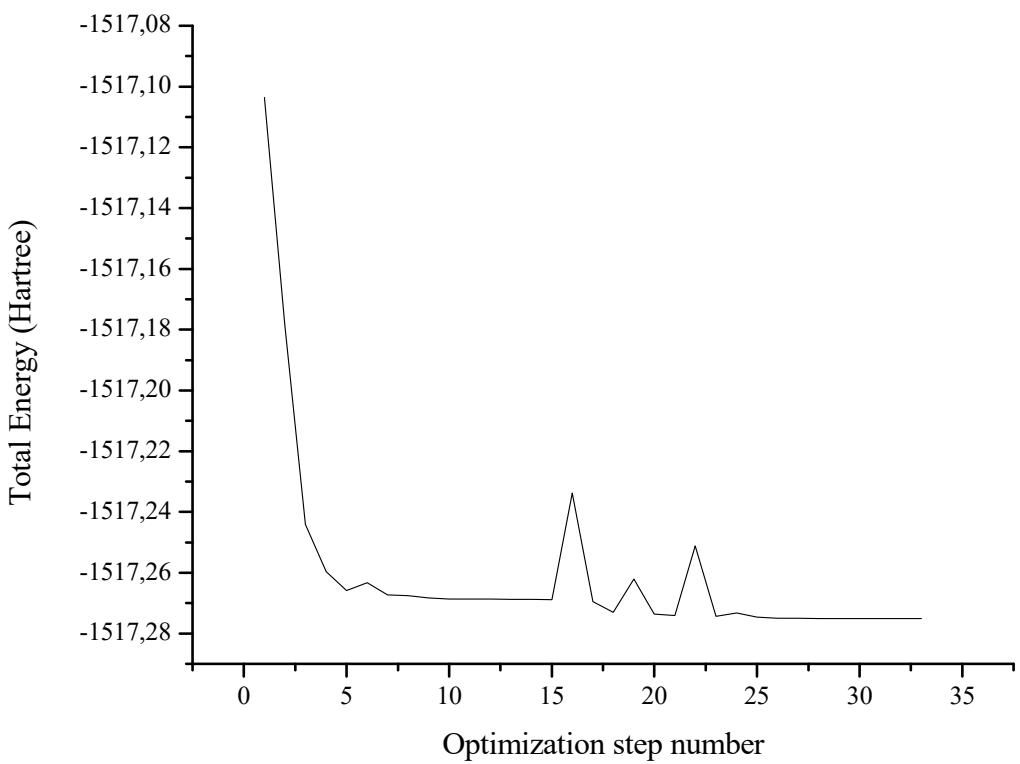
Tel.: +27(011)6709302



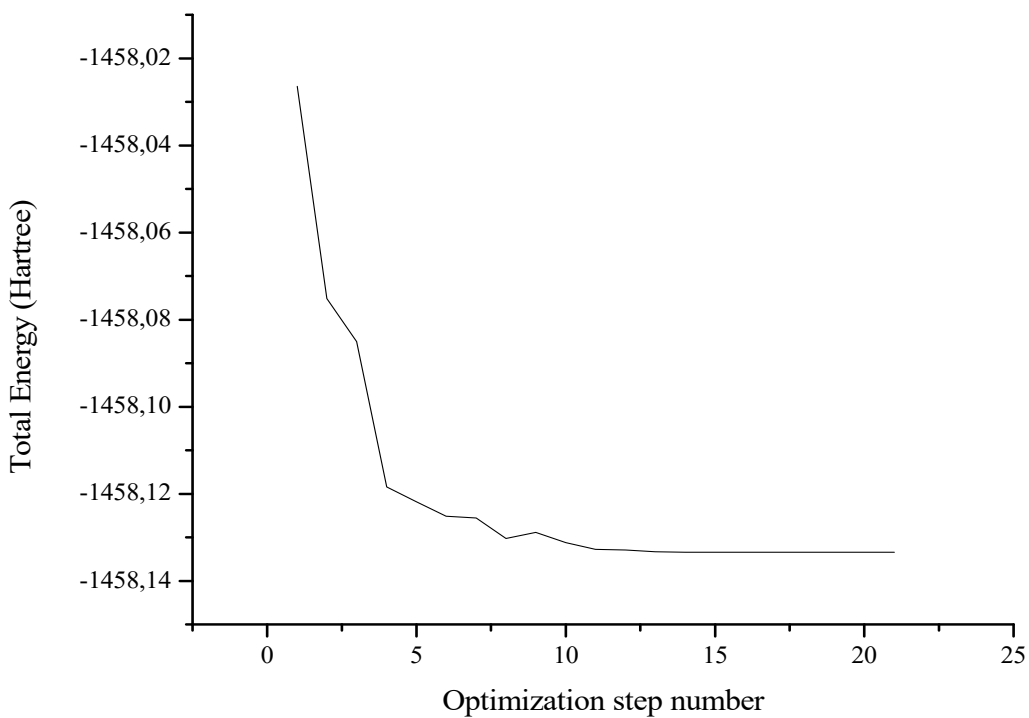
O1



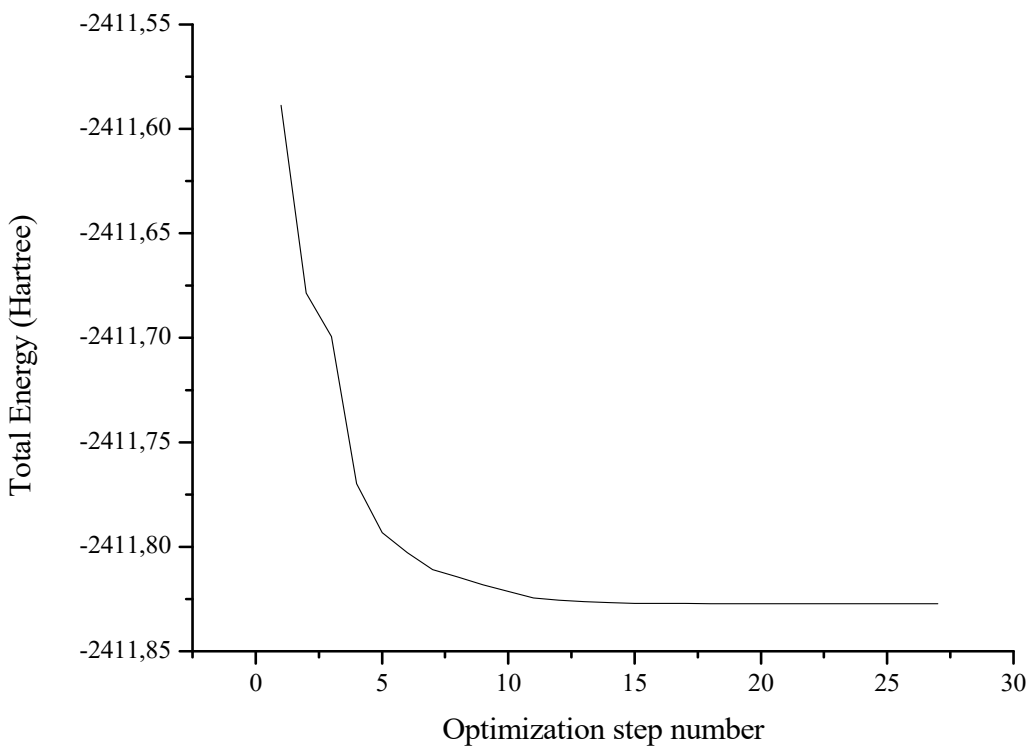
O2



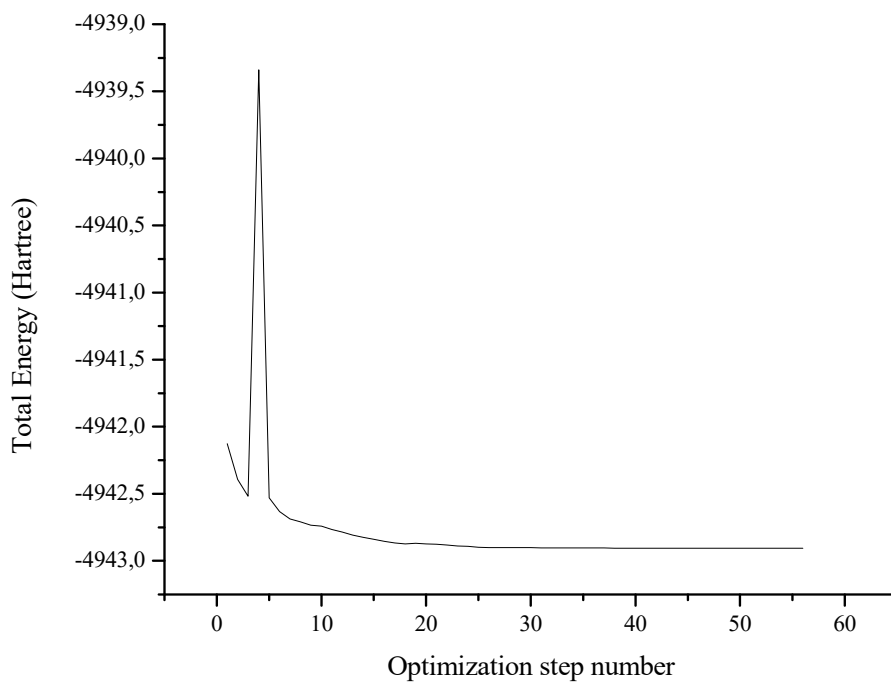
O3



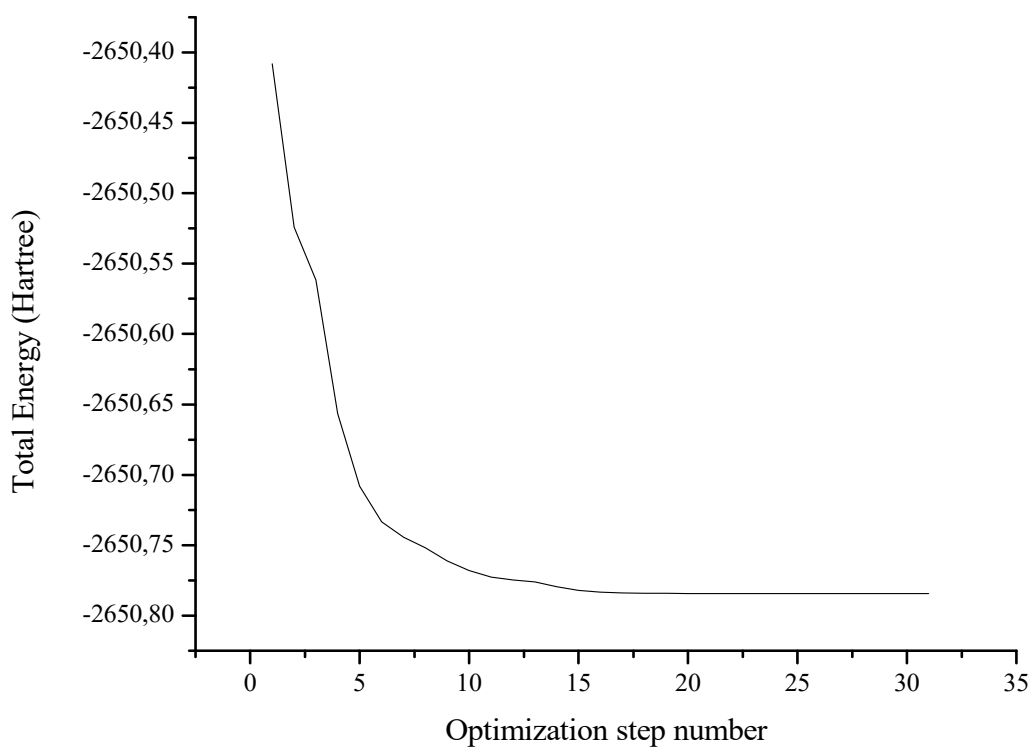
O4



O5

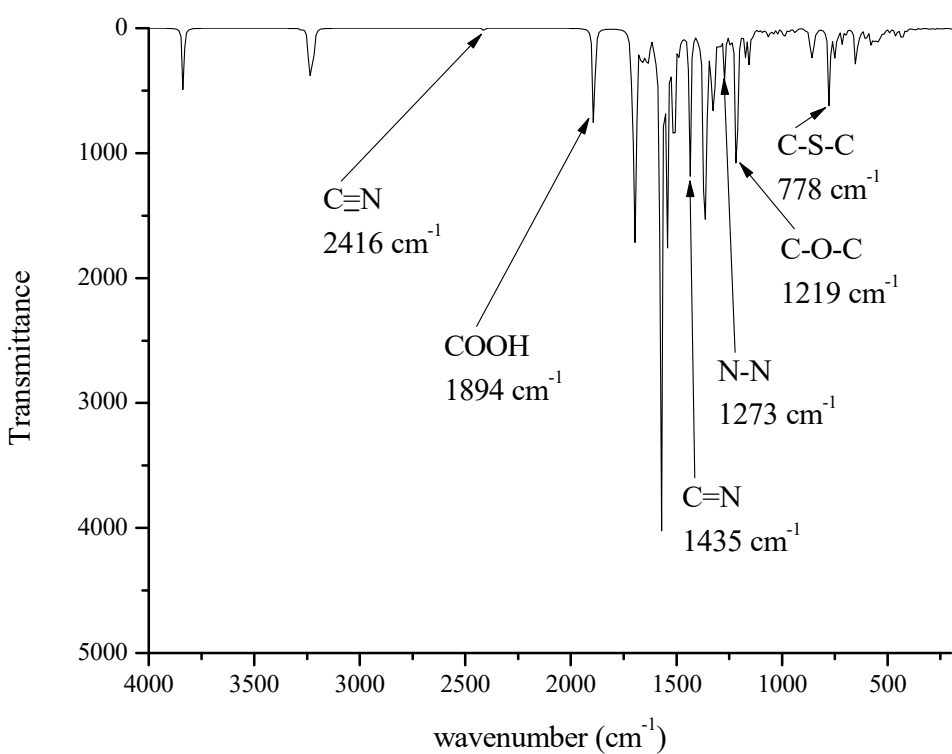


O6

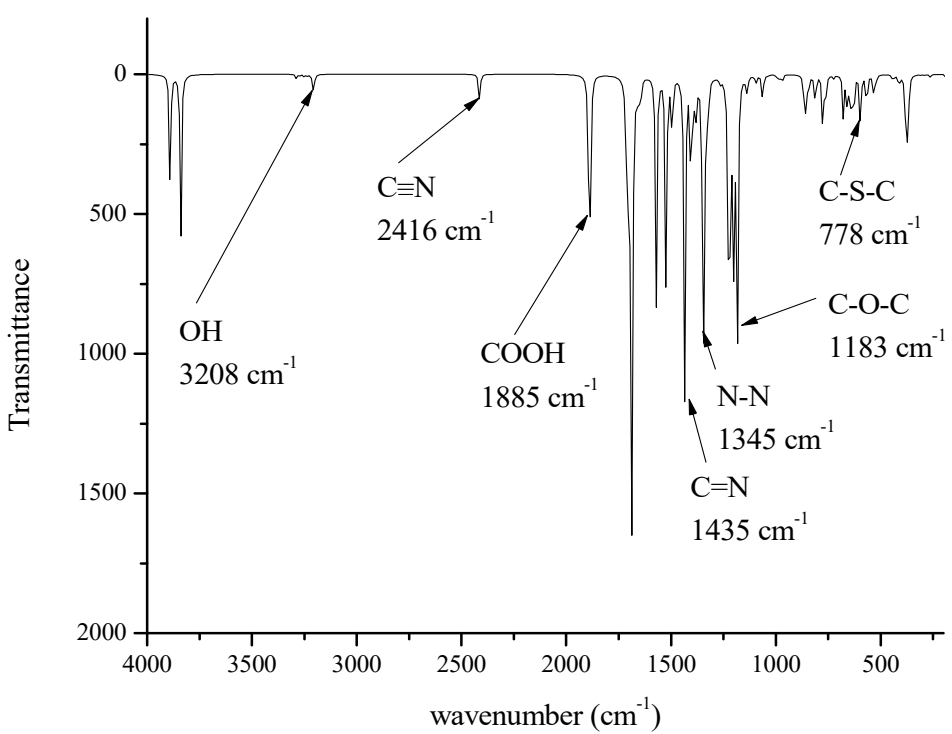


O7

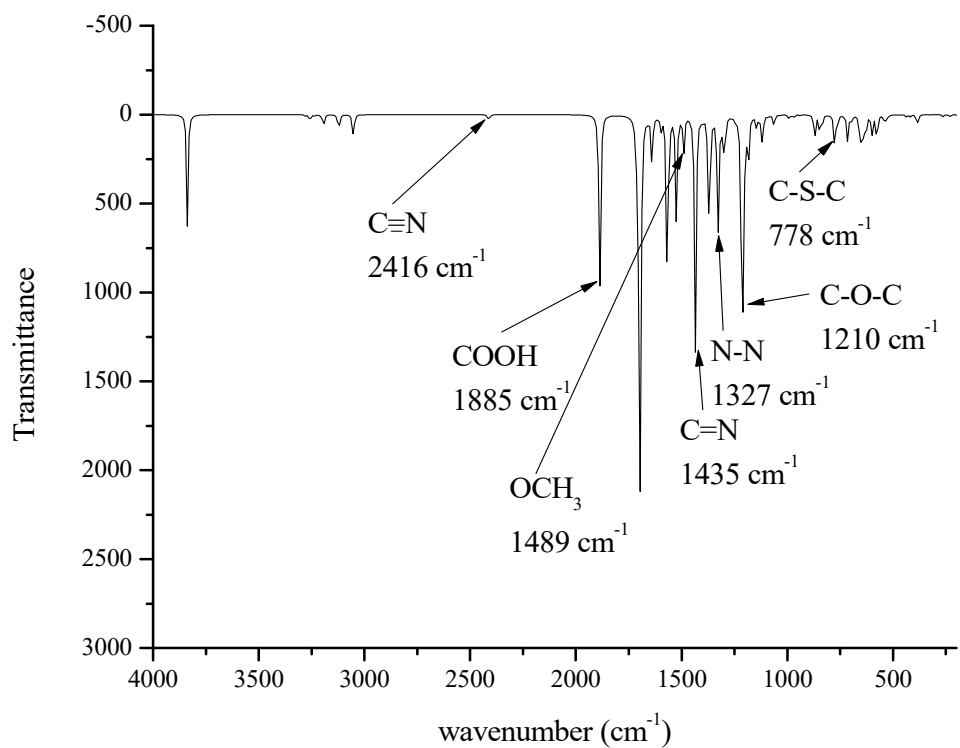
Figure S1: Optimization energies for the molecules obtained through DFT calculations



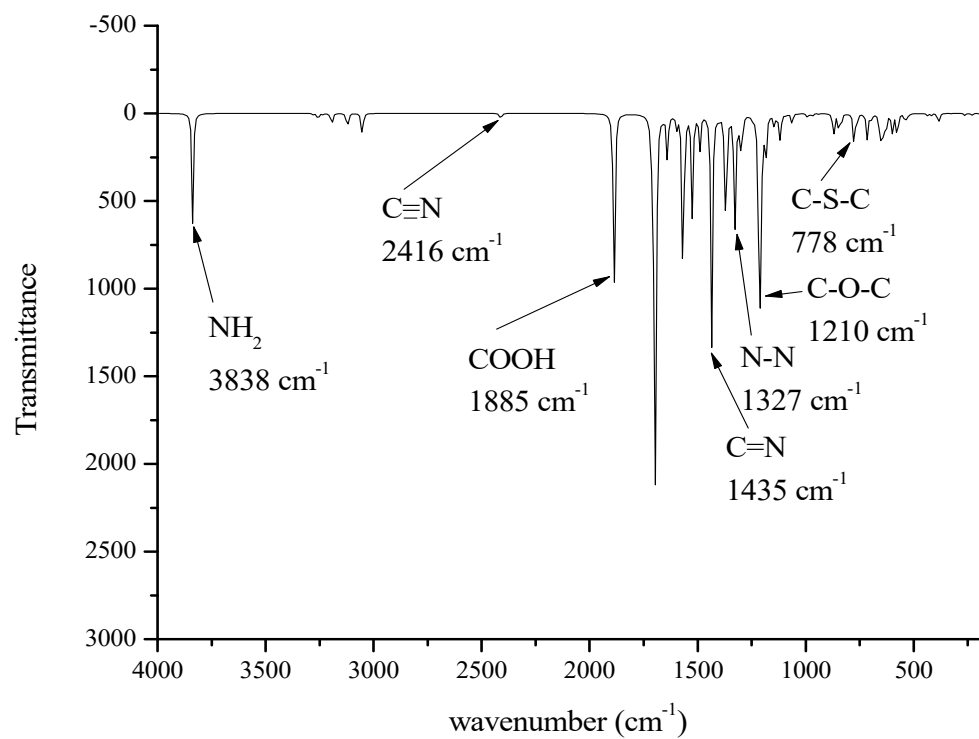
O1



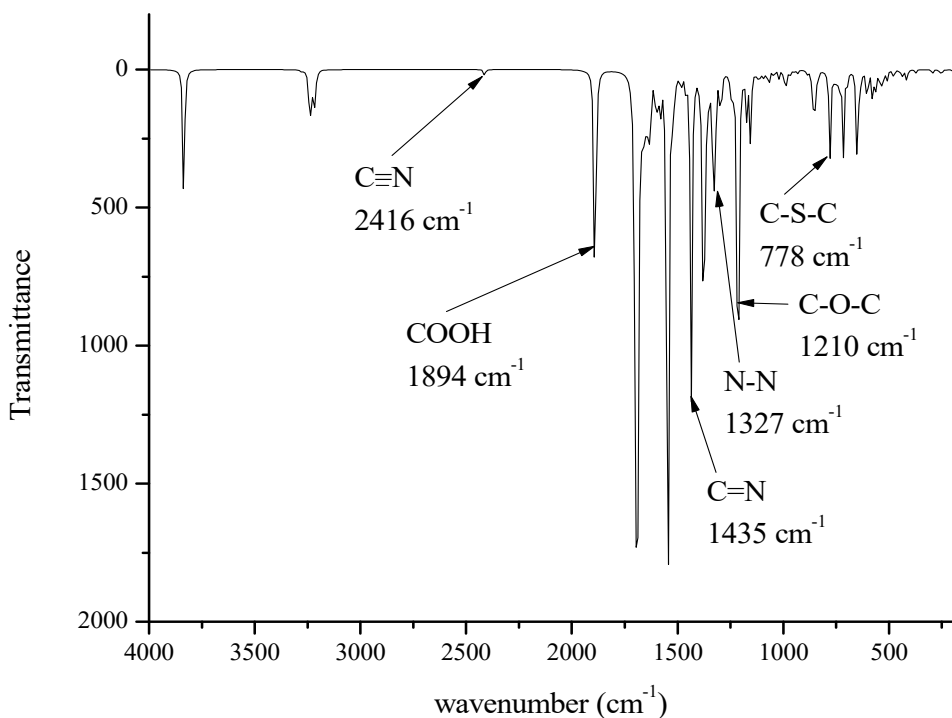
O2



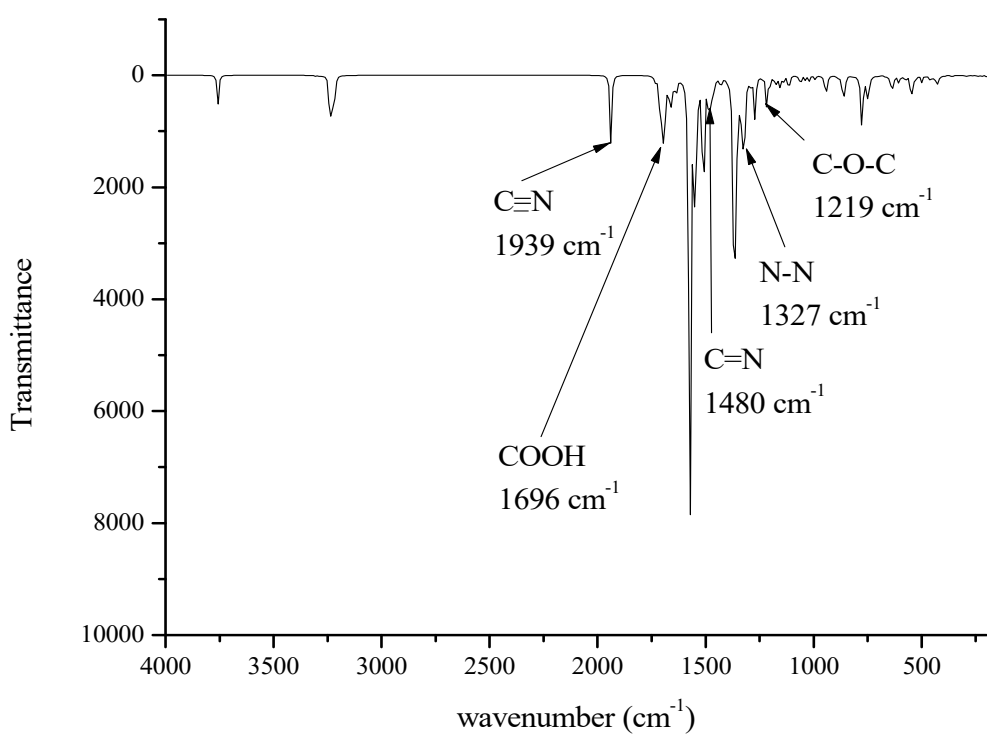
O3



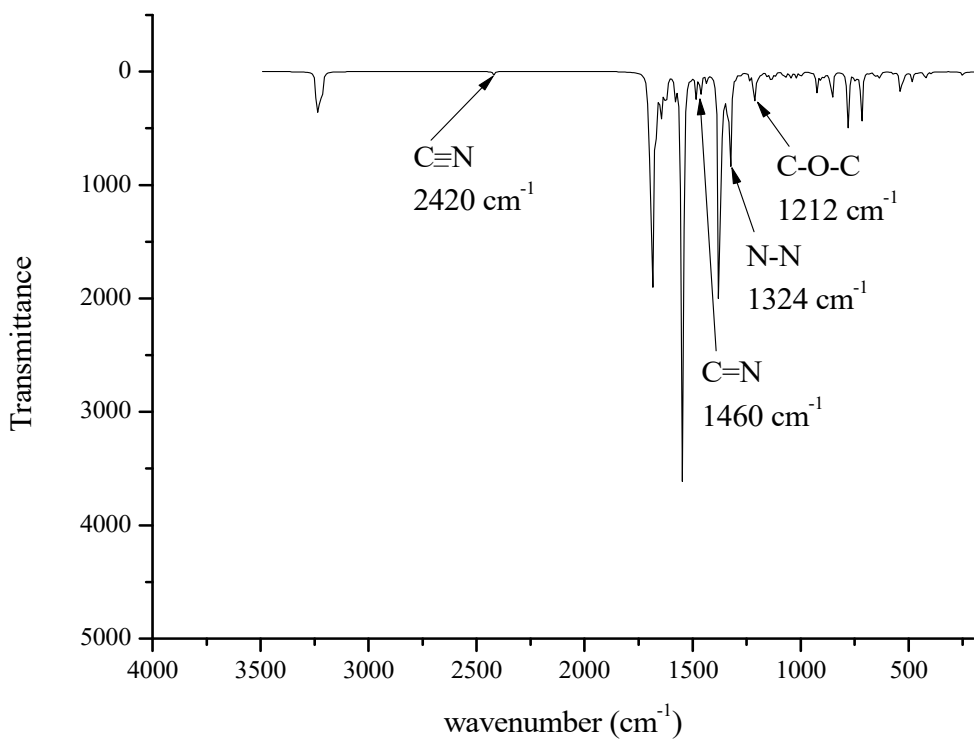
O4



O5



O6



O7

Figure S2: Computed IR spectra of 1,3,4-oxadiazoles

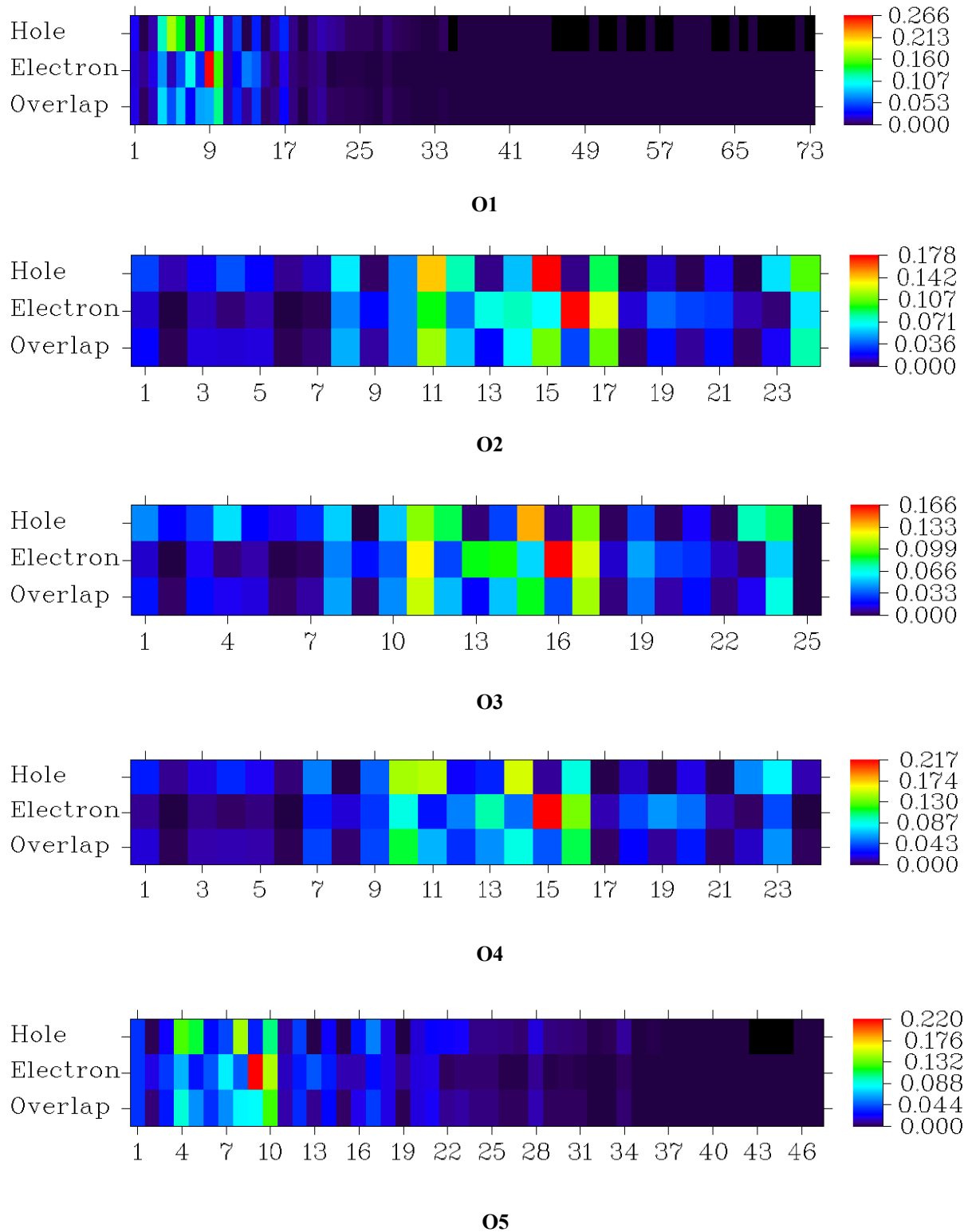
Atom based electron-hole analysis

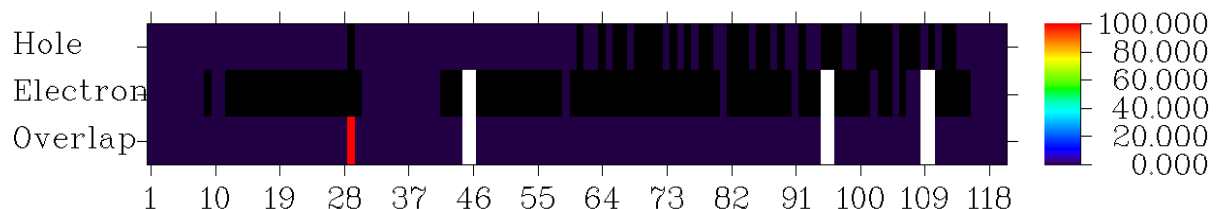
Figure S3 describes the contribution of each non-hydrogen atom to each hole, electron and overlap distributions. The hydrogens were omitted from this analyses as they yield negligible contributions. The values in the y-axis on the right hand side represents the fraction of the contribution from each atom in the abscissa. The assigned colour depends on the fraction of the contribution from each. The red represents the highest contribution, while dark blue represents the least contribution. The numbers in the abscissa represent the index for each atom within the molecule. The structures of each compound with its atomic code that corresponds to the atomic indexes in Figure S3 are given in Figure S4. The analyses on all the compounds were performed for the first excited state only. The two connected carbon atoms C5 and C7 that comprises the thiophene ring contributes substantially to holes and electrons (Figure S5). As the sum of their “Difference” is -6.46% (Table S1), which corresponds to their charge density difference (CCD), it implies that these two atoms loses 6.46% electrons during excitations. As C9, C11 and C13 comprises the acceptor fragment, we found that C9

contributes substantially to holes, while C11 and C13 contributes substantially to electrons. The “Difference” between electrons and holes in C9 of -10.18% indicates a loss of electrons during excitations, while the sum of the “Difference” of the combination of C11 and C13 of 28.79% reveals an increase in electron density during excitation. This is expected since C9 forms part of the thiophene ring [1-7], while C11 and C13 forms part of the acceptor fragment [7-11]. The sum of the “Difference” of -1.43% in the combination of C14 and N15 indicates that this group loses 1.43% electrons during excitations. As this group acts as an anchoring group that can inject electrons into the conduction band of the semiconductor [12-14], the loss of electrons means that it lacks electrons for injection. However, the sum of the “Difference” for the combination of C16, O17 and O18 is 8.05%. This gain in electrons during excitations is useful since it also acts as an anchoring group [12-14]. When an electron gets excited then it usually occupies the LUMO, while instantaneously leaving a hole behind in the HOMO or any other contours of atomic space where it used to be located. This also instantly forms an exciton due to a strong Coulomb interaction between the electron and the hole [15, 16]. Excitons can usually be excited in singlet (S) or triplet (T) spin configurations. The former results from opposite spins ($\uparrow\downarrow$ or $\downarrow\uparrow$) with a multiplicity of +1, while the latter results from parallel spins ($\uparrow\uparrow$ or $\downarrow\downarrow$) with a multiplicity of +3. The excitation selection rules for organic compounds only allow S excitons, and since all our compounds under study are organic, only S excitons will be considered. The exciton first relaxes to the ICT state by transferring its energy from the LUMO of the donor fragment to a lower energy level of the LUMO of the π -spacer fragment, and the excess energy is then released in the form of molecular vibrational energy. If this energy is larger than the exciton binding energy, then it can be transferred back into the ICT exciton to dissociate it into another pair of free electron and hole. Thus, it is critical that all generated excitons reach the interface between fragments within a dye for ICT so that the exciton can dissociate into free carriers, which can be collected at the interface between the dye and the semi-conductor. For free carriers to form, the ICT excitons must be long-lived. If it does not have a long-live state, then the free electron can recombine with the hole, which results in energy loss and decrease the efficiency of the dye. The Langevin theory states that charge recombinations in organic systems occurs when an electron and a hole are within the very short Coulomb radius from each other [17, 18]. This also result in large electron-hole overlaps. A large overlap occurs in the CN anchoring group, which is even larger than the electron contributions. This supports our earlier analyses that revealed that it lacks free electrons for injection into the semi-conductor. A much smaller overlap is observed for the COOH anchoring group, which also support our earlier observation. Table S2 indicates that C16 and C21 that

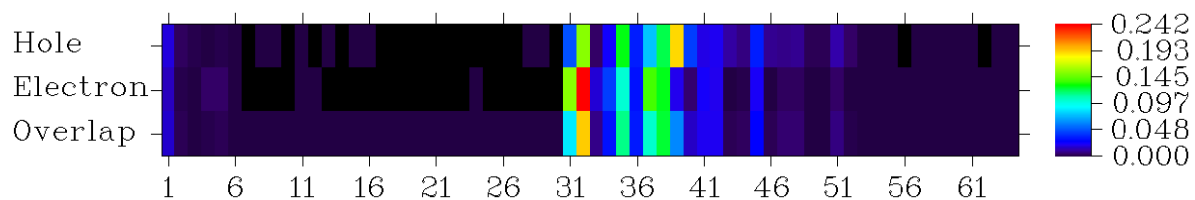
forms part of the thiophene ring in **O2** loses electrons, while C23, C25, C26 and C28 that forms part of the acceptor fragment gains electrons during excitations. It is C23 in particular that gains a substantial amount of electrons of 17.02%. This can also be seen in Figure S5. The anchoring groups CN and COOH receives 5.09% and 5.29% electrons during excitation. This means that the presence of the donor OH group transfers more electrons to the CN anchoring group but less electrons to the COOH anchoring group in this **O2** than the starburst moiety in **O1**. The OH moiety loses 0.97% electrons during excitation though as a result of its donating ability. Less electron-hole overlaps are also observed for the CN and COOH anchoring groups, which also supports our analyses for the observation of the concentration of electrons for these groups. Table S3 indicates that the OCH₃ moiety in **O3** donates less electrons of 0.69% during excitation. Figure S5 shows that electrons are mainly localize on C22. The cyano anchoring group gains 2.56% electrons, while the COOH anchoring groups gains 4.55% electrons during excitations. The NH₂ moiety in **O4** donates more electrons (1.09%) during excitations than the OH and OCH₃ moieties as shown in Table S4. Figure S5 shows that the atoms that comprises the π -spacer fragment, namely C14, C15 and C19 loses large amounts of electrons. Most electrons are delocalize to C21 with 20.8% and a substantial amount is also delocalize to C23 (4.69%) from the π -spacer fragment. The CN and COOH anchoring groups also receive a substantial amount of electrons of 3.68% and 9.74% each during excitations. The smaller electron-hole overlaps for these anchroing groups than their electron contributions further supports this. In **O5**, C4 (-6.05%), C5 (-8.50%) and C9 (-10.12%) loses a substantial amount of electrons during excitations (Table S5). The CN anchoring group loses electrons (-0.44%), while the COOH anchoring group gains 3.36% electrons during excitations. A slightly larger electron-hole overlap (4.54%) than the electron contribution (4.37%) for the CN anchoring group, while a smaller electron-hole overlap (5.46%) than electron contribution (8.71%) confirm our findings. A large amount of electrons (35.77%) in **O6** are excited to C47, while C48 loses 5.58% electrons due to excitations (Table S6). The CN anchoring group also receive a large amount of electrons (27.06%), while the COOH group receive a reasonable amount of electrons (6.83%) during excitations. This is also confirmed by the much smaller electron-hole overlap for the CN anchoring group (15.38%) than its electron contribution (38.12%), and the smaller electron-hole overlap for the COOH anchoring group (2.6%) than its electron contribution (7.81%). The two connecting atoms C49 and C50 in **O7** receives 10.61% and 8.67% electrons each during excitations (Table S7). As only a CN anchoring group is present in this compound, this anchoring group receives 3.29% electrons during excitations. The smaller electron-hole overlap for this anchoring group (3.05%) than its electron contribution

(6.80%) also confirm our findings. Based on these analyses, the anchoring groups of the molecules with the largest concentration of electrons lies in the order **O6>O4>O2>O1>O3>O7>O5**.



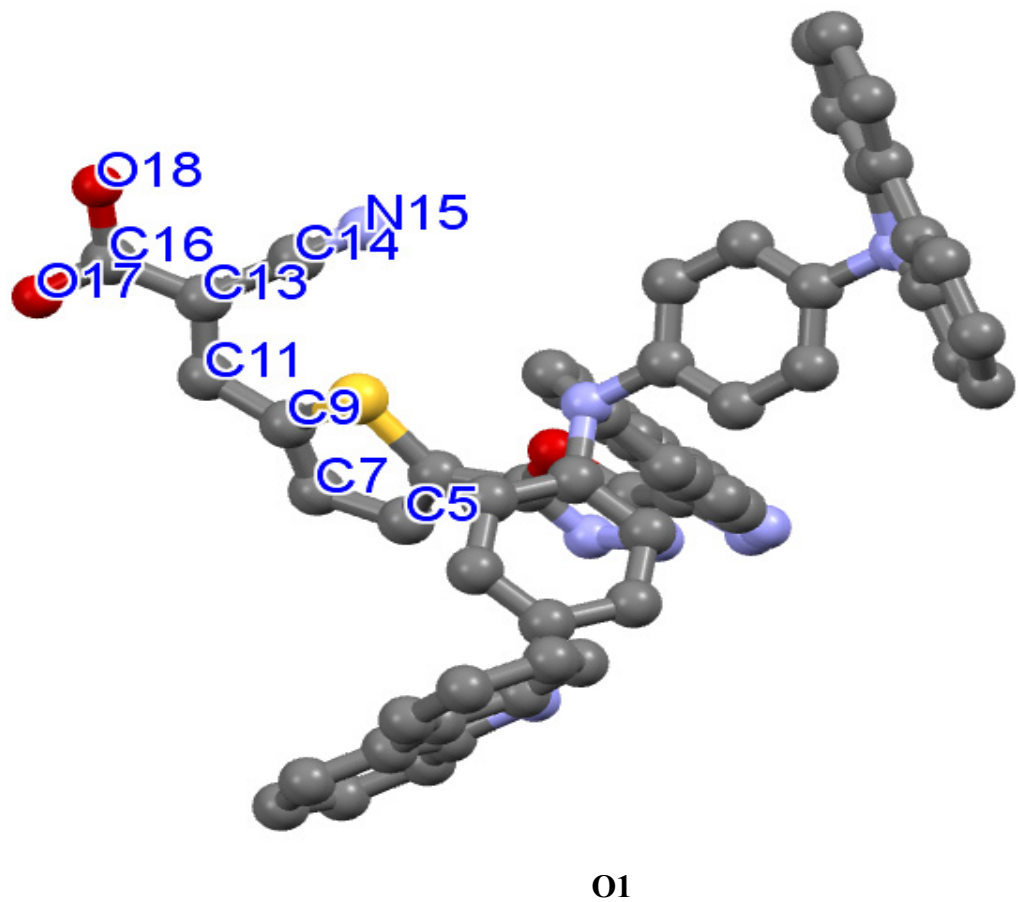


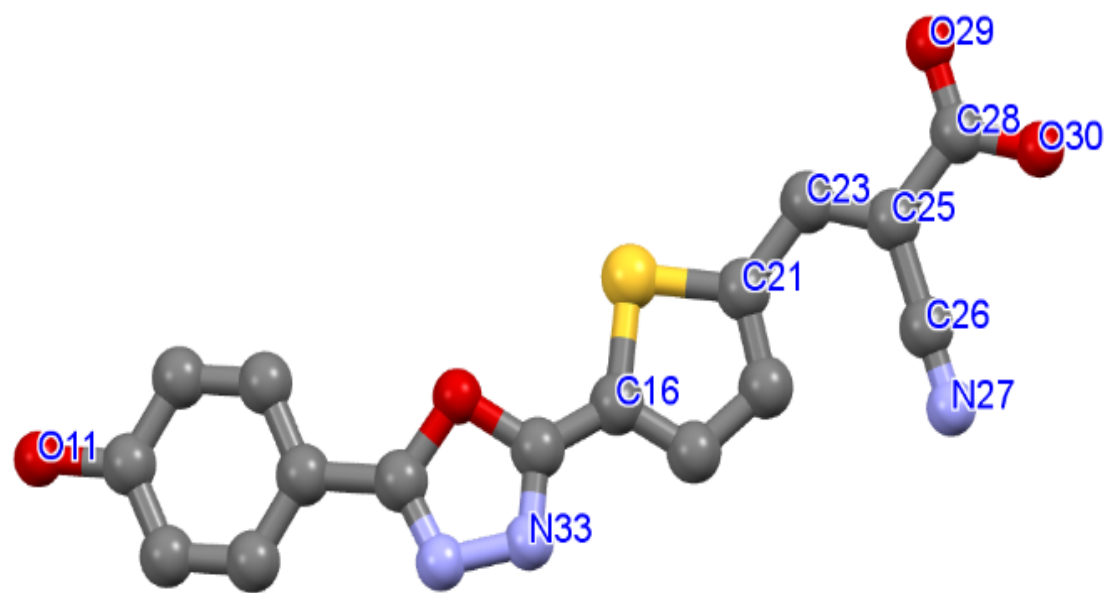
O6



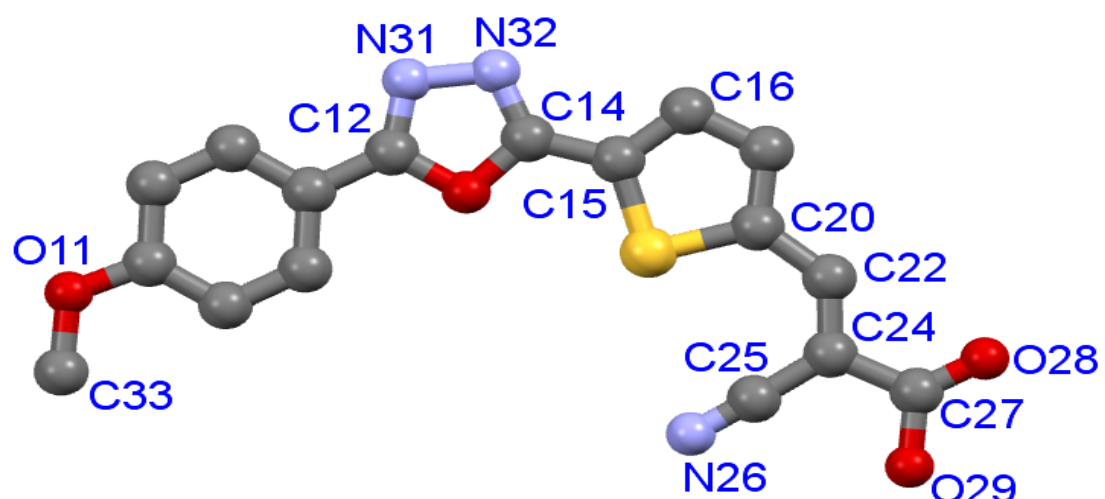
O7

Figure S3: Electron excitation in each non-hydrogen atom of each molecule

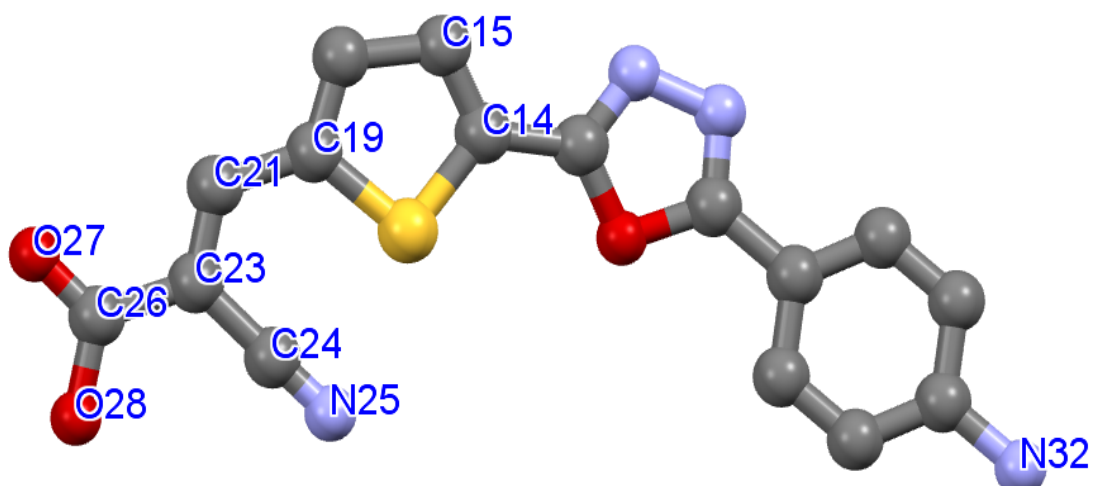




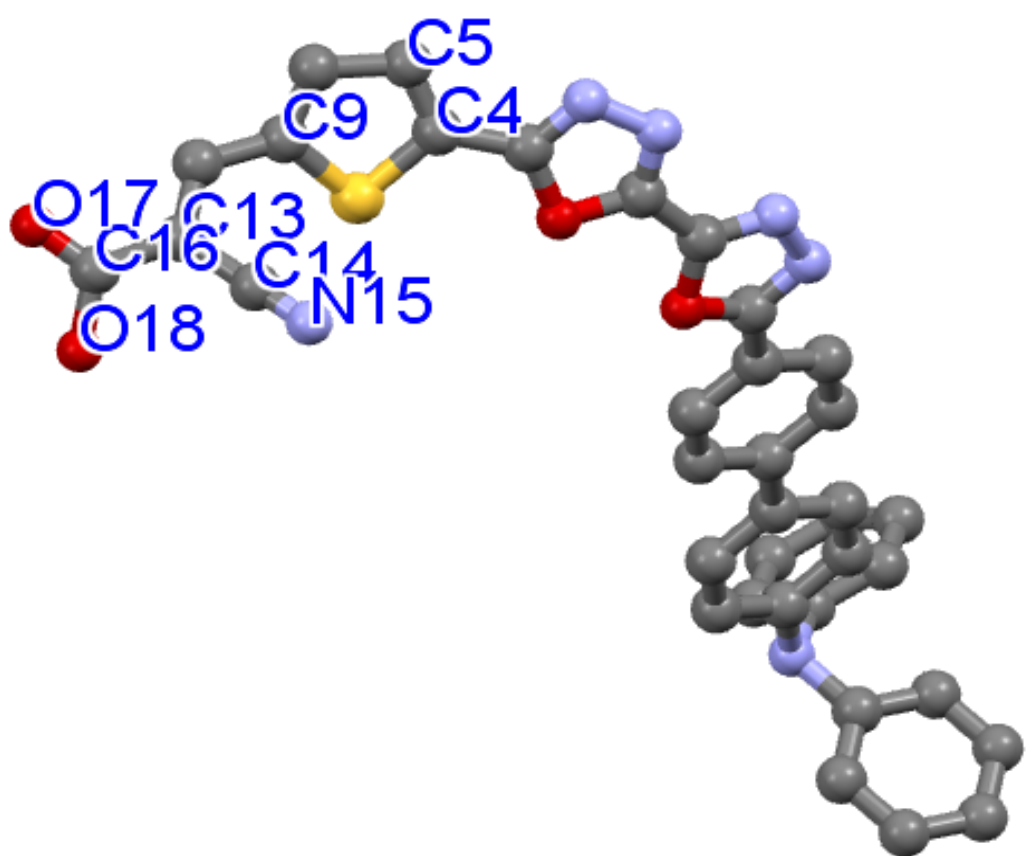
O2



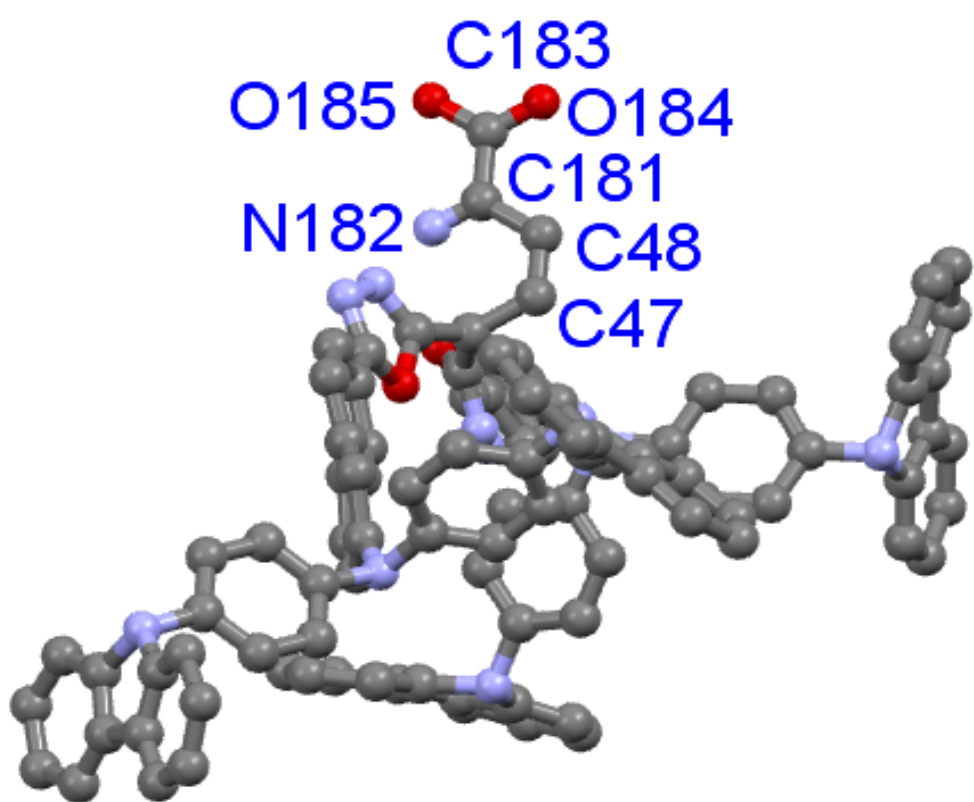
O3



O4



O5



O6

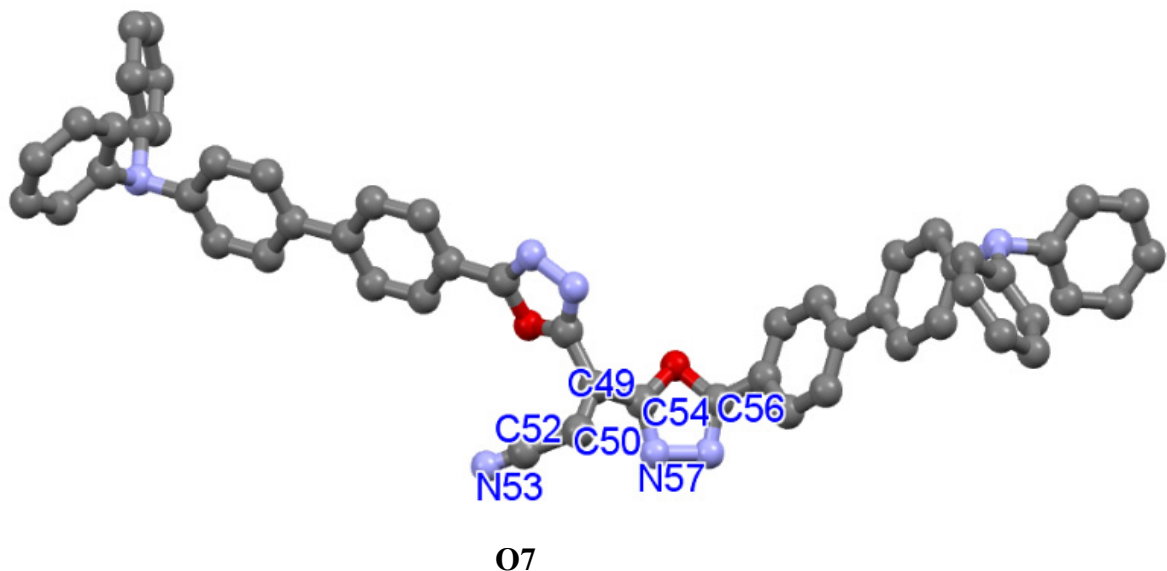
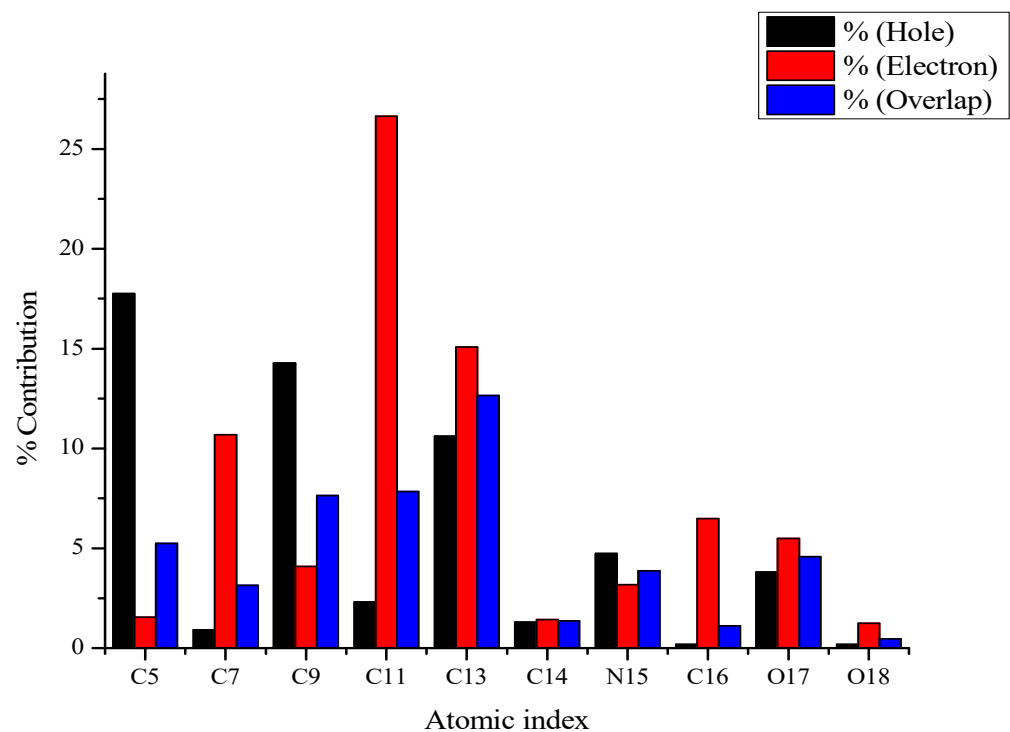
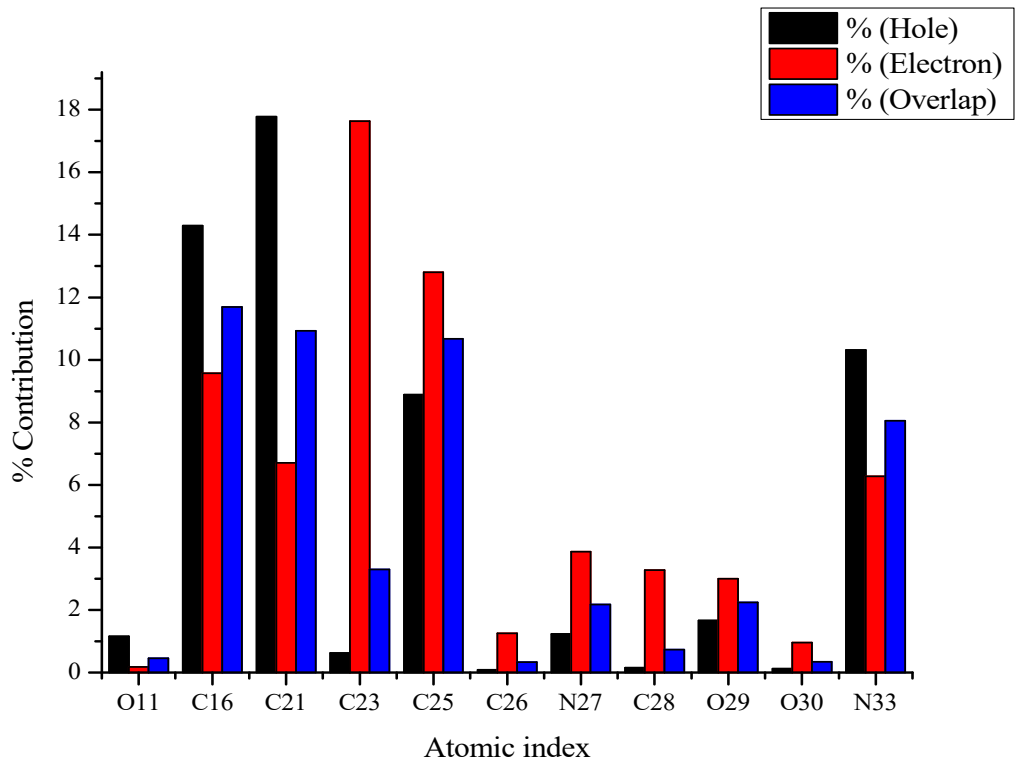


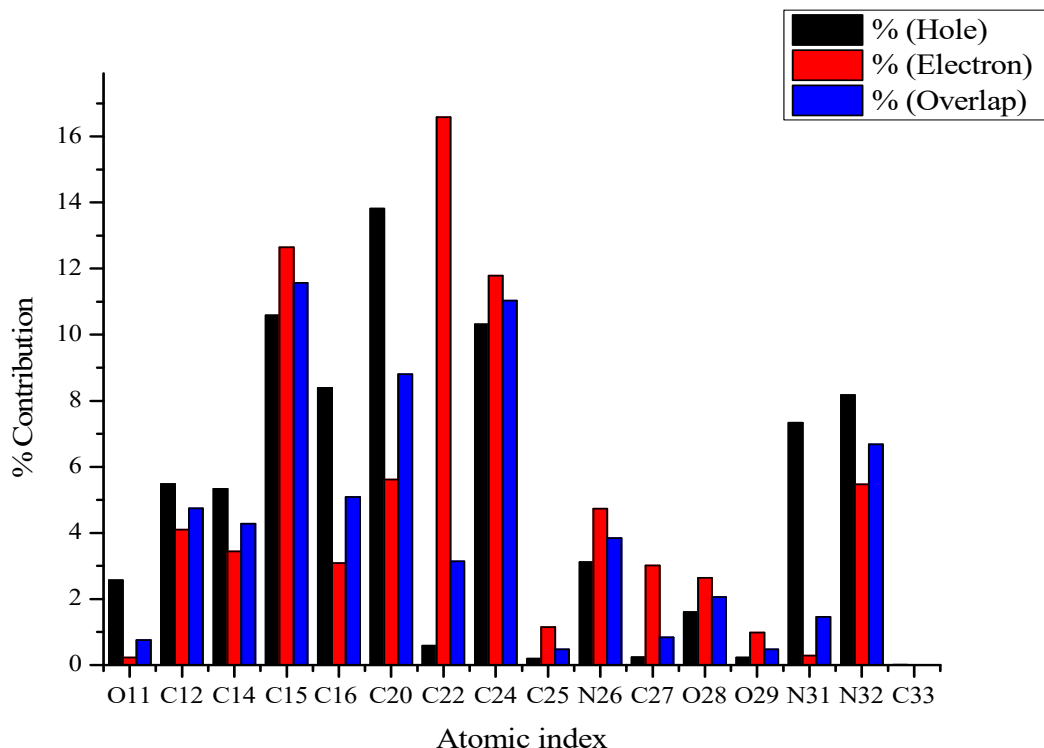
Figure S4: Molecular structures of each molecule optimized through Gaussian and obtained from Mercury 2020



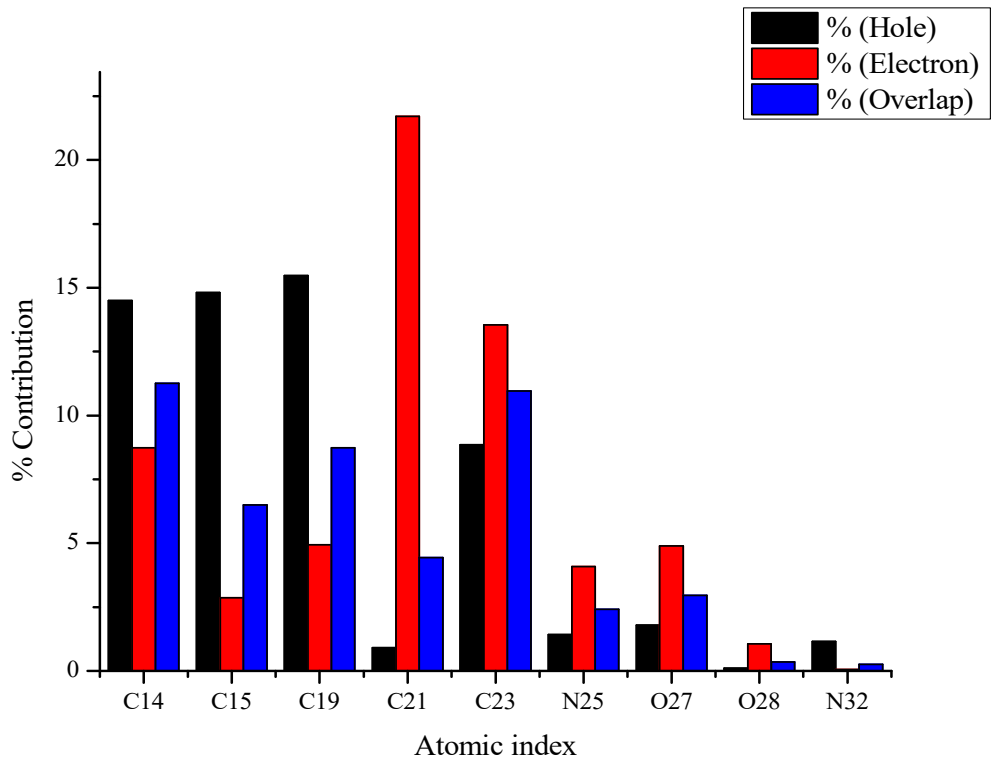
O1



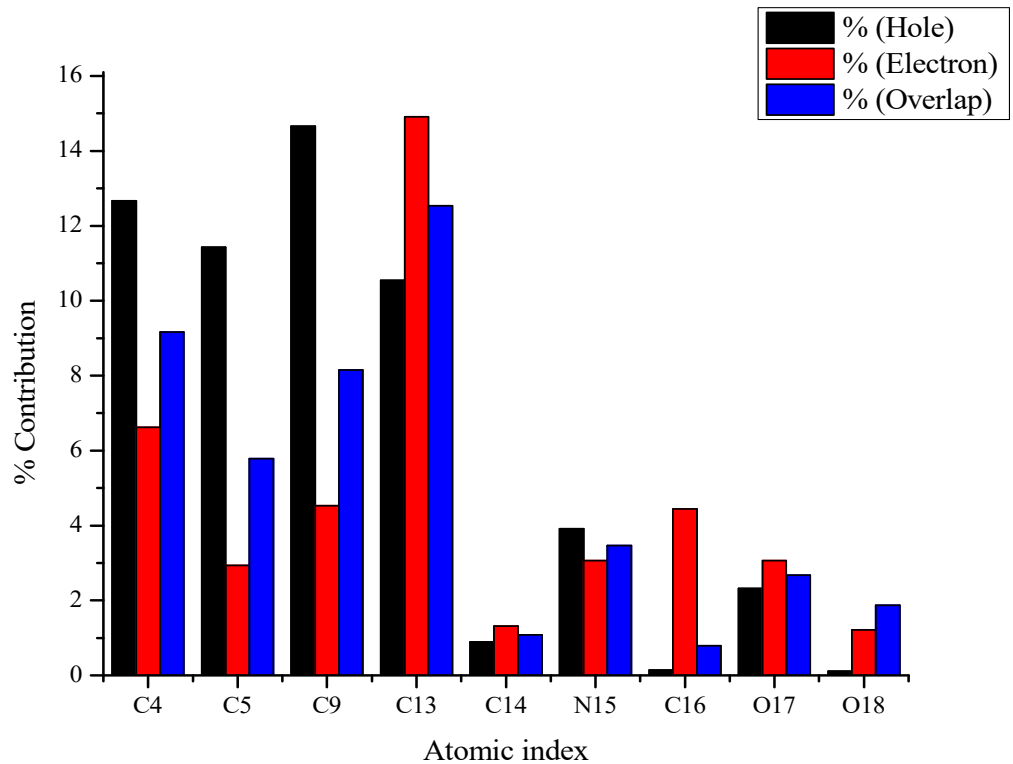
O2



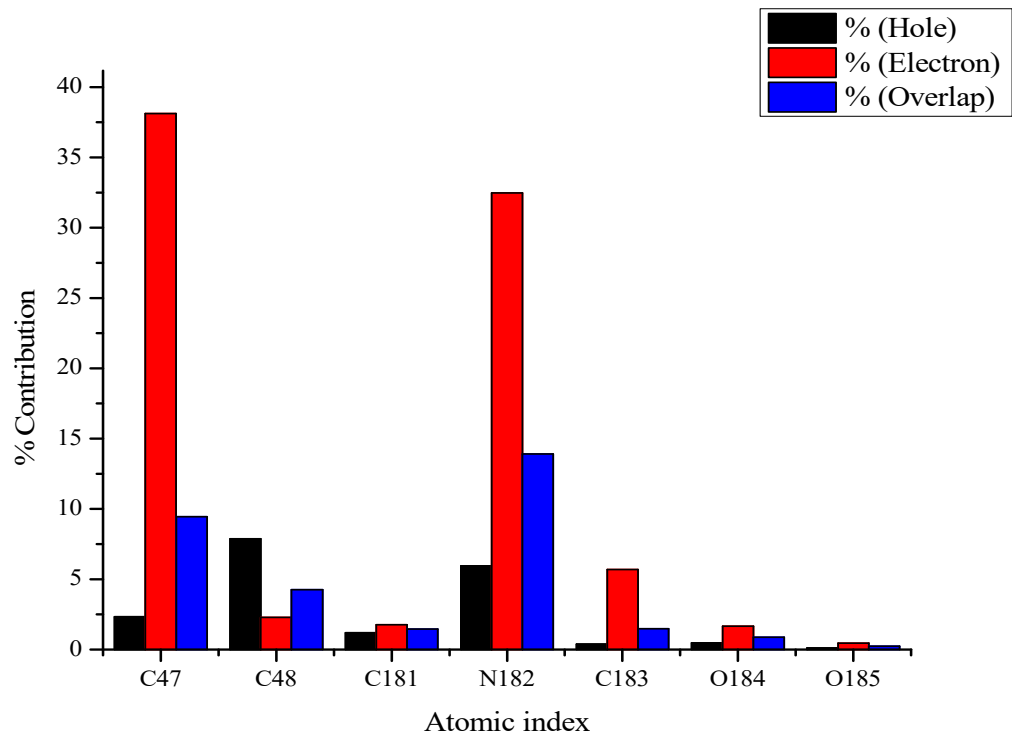
O3



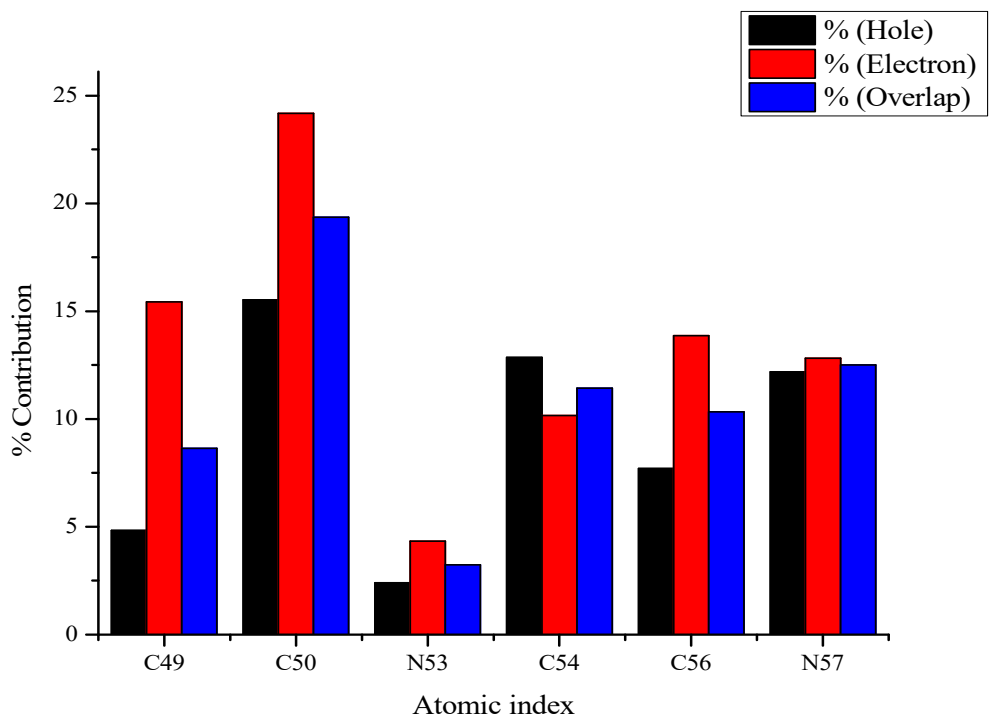
O4



O5



O6



O7

Figure S5: Electron-hole contribution analyses of each non-hydrogen atom

Table S1: Contribution of each selected non-hydrogen atoms to hole and electron within **O1**

	Hole (%)	Electron (%)	Overlap (%)	Difference (%)
C5	17.76	1.54	5.24	-16.22
C7	0.92	10.68	3.14	9.76
C9	14.27	4.09	7.64	-10.18
C11	2.31	26.64	7.84	24.33
C13	10.61	15.08	12.65	4.46
C14	1.29	1.43	1.36	0.14
N15	4.75	3.18	3.88	-1.57
C16	0.19	6.49	1.11	6.30
O17	3.81	5.49	4.57	1.68
O18	0.18	1.25	0.47	1.07

Table S2: Contribution of each selected non-hydrogen atoms to hole and electron within **O2**

	Hole (%)	Electron (%)	Overlap (%)	Difference (%)
O11	1.15	0.18	0.45	-0.97
C16	14.29	9.57	11.69	-4.72
C21	17.78	6.71	10.93	-11.06
C23	0.62	17.64	3.30	17.02
C25	8.89	12.80	10.67	3.91
C26	0.09	1.26	0.33	1.18
N27	1.23	3.87	2.18	2.64
C28	0.16	3.28	0.73	3.12
O29	1.67	3.00	2.24	1.33
O30	0.12	0.96	0.34	0.84
N33	13.32	6.28	8.05	-4.04

Table S3: Contribution of each selected non-hydrogen atoms to hole and electron within **O3**

	Hole (%)	Electron (%)	Overlap (%)	Difference (%)
O11	2.57	0.23	0.76	-2.34
C12	5.48	4.10	4.74	-1.38
C14	5.33	3.44	4.28	-1.88
C15	10.58	12.65	11.57	2.07
C16	8.39	3.09	5.09	-5.30
C20	13.82	5.61	8.80	-8.21
C22	0.590	16.58	3.14	15.99
C24	10.32	11.79	11.03	1.470
C25	0.20	1.15	0.48	0.96
N26	3.12	4.73	3.84	1.60
C27	0.24	3.01	0.84	2.78
O28	1.61	2.64	2.06	1.02
O29	0.23	0.98	0.48	0.75
N31	7.33	0.29	1.46	-7.04
N32	8.17	5.47	6.68	-2.70
C33	0.01	0.00	0.00	-0.01

Table S4: Contribution of each selected non-hydrogen atoms to hole and electron within **O4**

	Hole (%)	Electron (%)	Overlap (%)	Difference (%)
C14	14.50	8.73	11.25	-5.77
C15	14.81	2.86	6.50	-11.96
C19	15.47	4.94	8.74	-10.52
C21	0.91	21.71	4.43	20.80
C23	8.86	13.55	10.96	4.69
C24	0.15	1.17	0.41	1.03
N25	1.43	4.08	2.41	2.65
C26	0.14	5.83	0.92	5.68
O27	1.79	4.90	2.96	3.11
O28	0.11	1.06	0.35	0.95

N32	1.15	0.06	0.26	-1.09
-----	------	------	------	-------

Table S5: Contribution of each selected non-hydrogen atoms to hole and electron within **O5**

	Hole (%)	Electron (%)	Overlap (%)	Difference (%)
C4	12.67	6.62	9.16	-6.05
C5	11.43	2.93	5.78	-8.50
C9	14.66	4.53	8.15	-10.12
C13	10.54	14.91	12.54	4.37
C14	0.89	1.31	1.08	0.41
N15	3.91	3.06	3.46	-0.85
C16	0.14	4.44	0.79	4.30
O17	2.32	3.06	2.67	0.74
O18	0.11	1.21	1.87	-1.68

Table S6: Contribution of each selected non-hydrogen atoms to hole and electron within **O6**

	Hole (%)	Electron (%)	Overlap (%)	Difference (%)
C47	2.34	38.11	9.45	35.77
C48	7.87	2.29	4.25	-5.58
C181	1.20	1.75	1.45	0.55
N182	5.96	32.46	13.91	26.51
C183	0.38	5.68	1.47	5.30
O184	0.47	1.67	0.89	1.20
O185	0.13	0.46	0.24	0.33

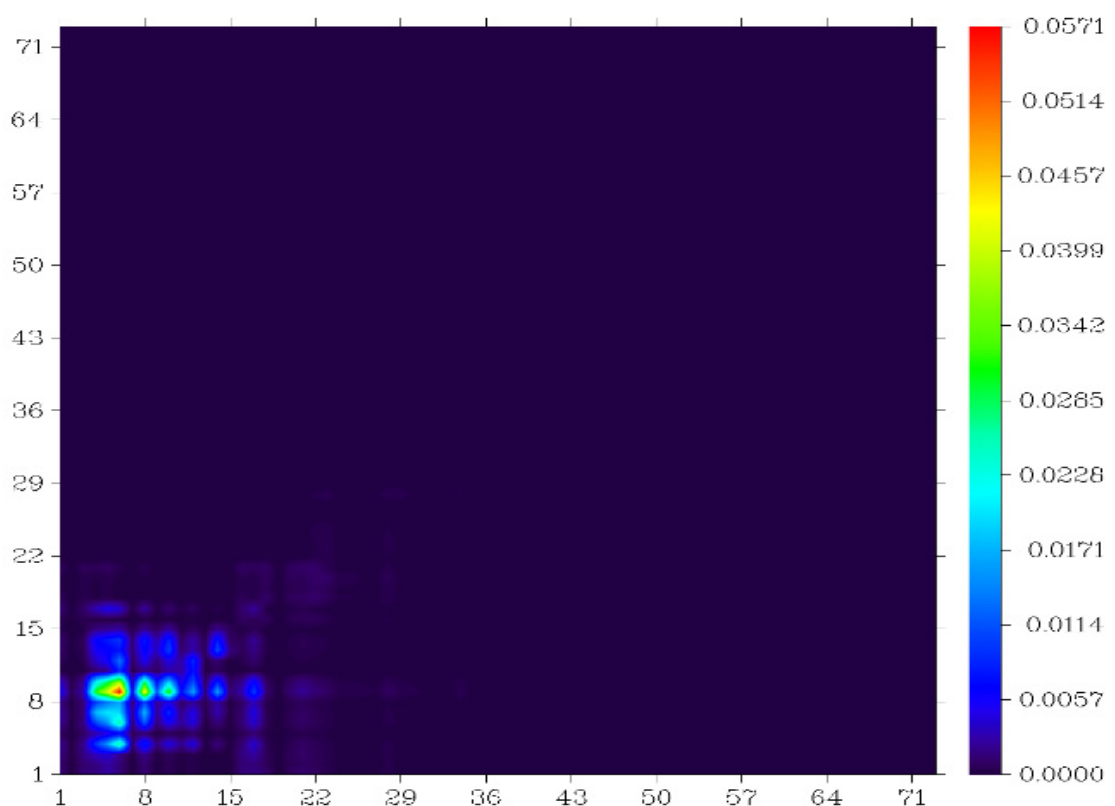
Table S7: Contribution of each selected non-hydrogen atoms to hole and electron within **O7**

	Hole (%)	Electron (%)	Overlap (%)	Difference (%)
C49	4.83	15.44	8.64	10.61
C50	15.52	24.18	19.37	8.67
C52	0.39	1.74	0.82	1.35
N53	2.40	4.34	3.23	1.94

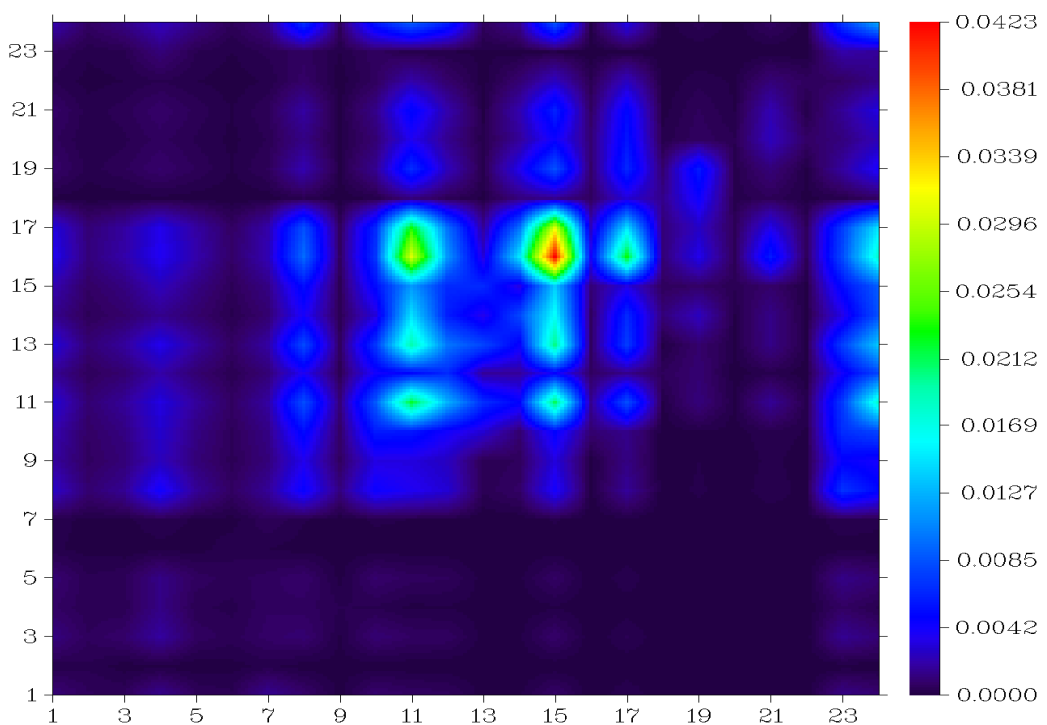
C54	12.86	10.17	11.44	-2.69
C56	7.70	13.86	10.33	6.16
N57	12.19	12.83	12.51	0.64

Transition density matrix of atom-based analysis

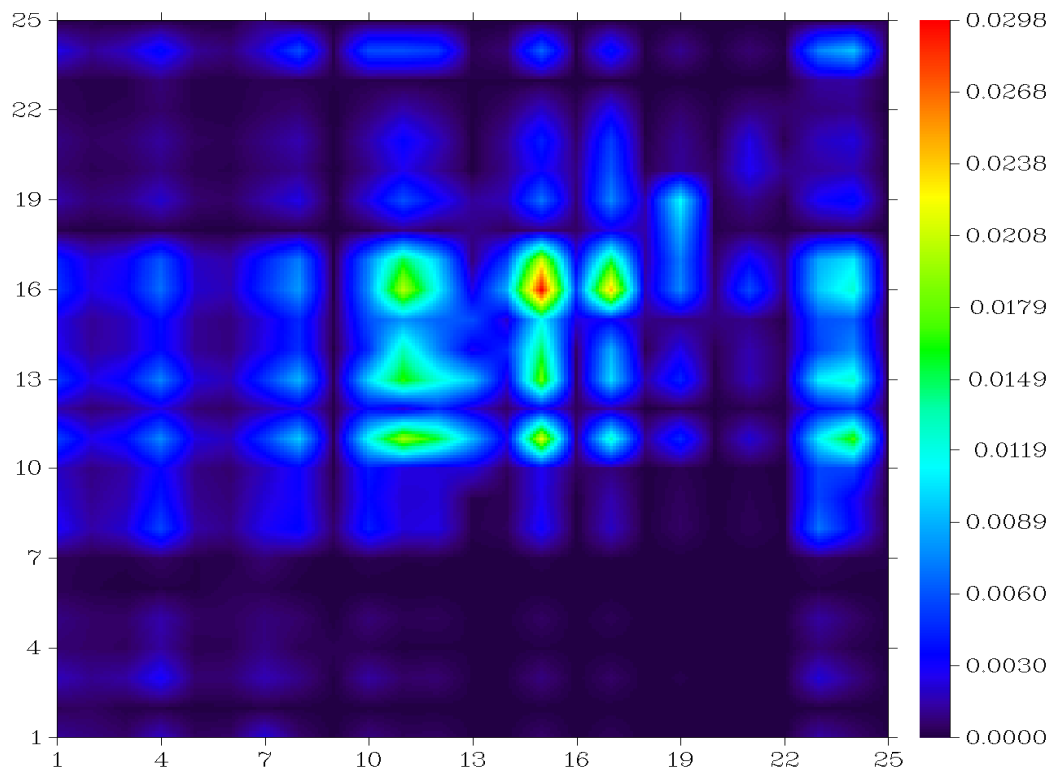
The electron concentrations for the atomic index are located on the y-axis, while the hole distributions for the atomic index is located on the x-axis in Figure S6. A quantitative analysis of electron-hole distributions is displayed in Tables S1-S7. No symmetrical distribution of electrons is observed in **O1**. The green and red colours in the x-axis that corresponds to C5, C9 and C13 results from holes that are generated from excited electrons. The red colour that corresponds to C5 indicate that this atom excites a larger number of electrons. The red colour corresponds to C11 in the y-axis. This means that many electrons that gets excited from C5 are transferred to the LUMO level of C11, while the rest will be transferred to the LUMO levels of C7 and C13. Electrons that are excited from C9 will also be transferred into the LUMO levels of these atoms. However, as C13 shows green colours for both holes and electrons, a large electron-hole overlap across this atom occurs but might not be large enough to prevent charge recombination. Many electrons get excited from C16 and N33 in **O2**, which will subsequently be transferred to the LUMO levels of C23 and C25. However, large electron-hole overlaps are observed for C16, C21 and C25. Amongst the atoms within **O3**, most electrons are excited from C15, C20 and C24, of which most of them are transferred to the LUMO levels of C22, and a substantial number to the LUMO levels of C15 and C24. The large electron-hole overlaps for C15 and C24 means a high probability for charge recombination within these atoms. Several other atoms that include C12, C14, N26 and N32 also shows large electron-hole overlaps. Many electrons from the atoms C14, C15 and C19 in **O4** are excited. Upon excitation, many of them are transferred to the LUMO levels of C21 and C23. However, large electron-hole overlaps are also observed for C14, C19 and C23. By observing **O5**, many electrons from C4, C5, C9 and C13 are excited. A large number is transferred back to C13 upon excitation. Thus, a large electron-hole overlap occurred within this atom. In **O6**, it is C48 and N182 that predominates with regards to excitations. Most of the electrons are transferred to the LUMO levels of C47, N182 and C183. Large electron-hole overlaps occurred in C47 and N182. In **O7**, C49 and C50 experiences most excitations. Upon excitation, most of the excited electrons are transferred to the LUMO levels of these same atoms, resulting in large electron-hole overlaps.



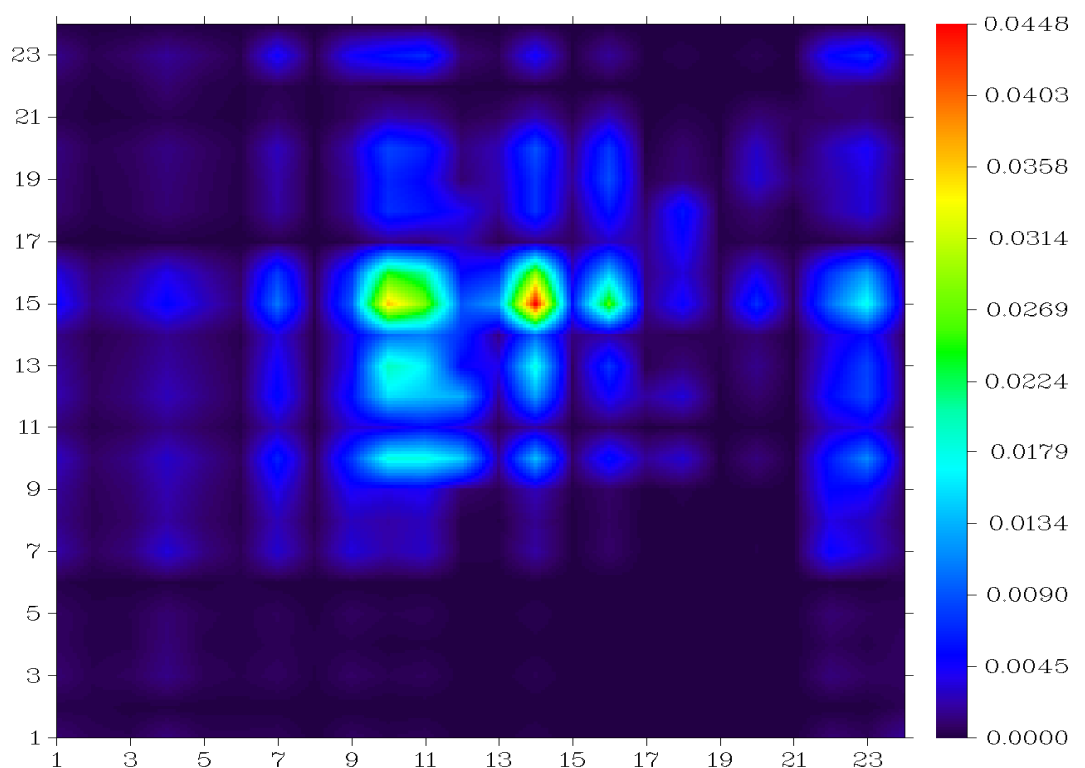
O1



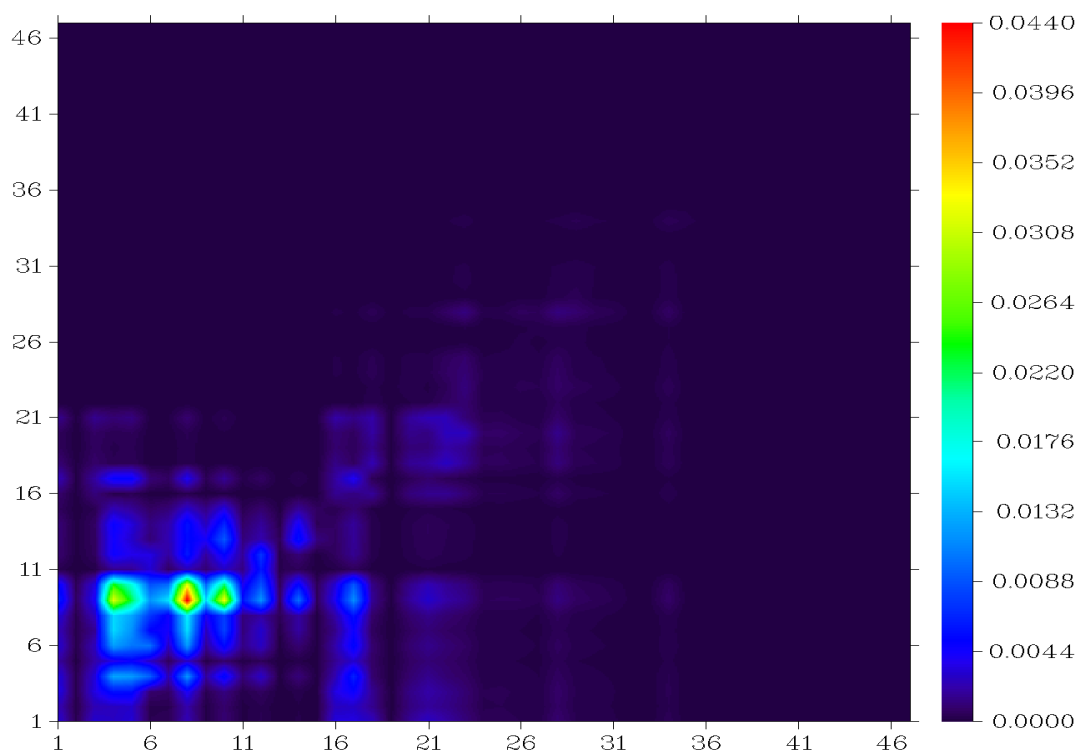
O2



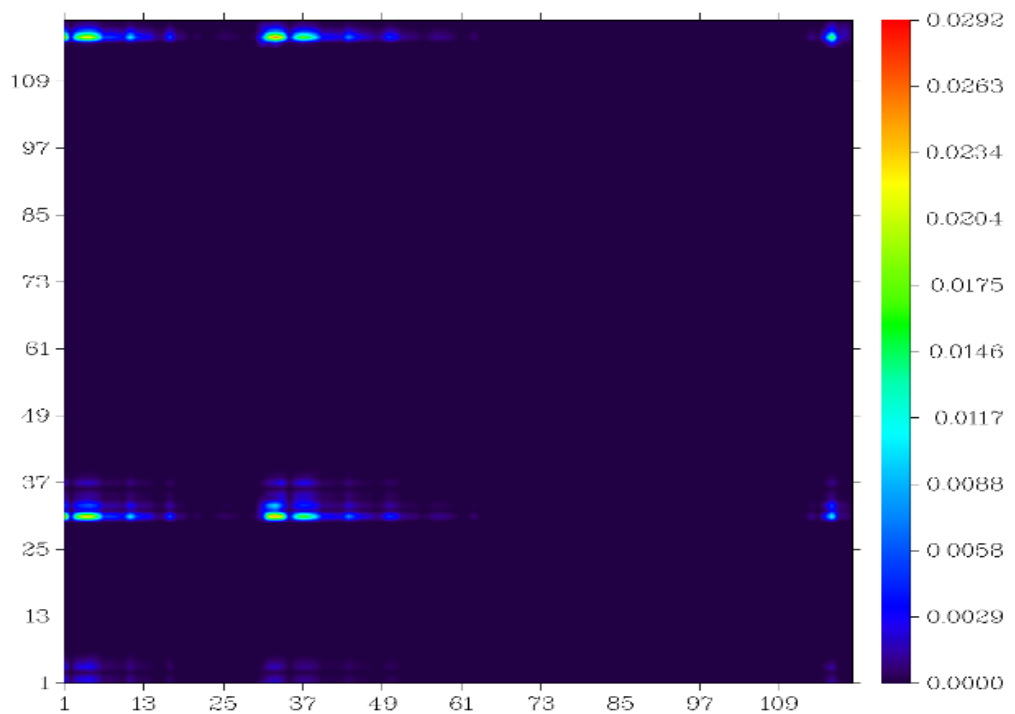
O3



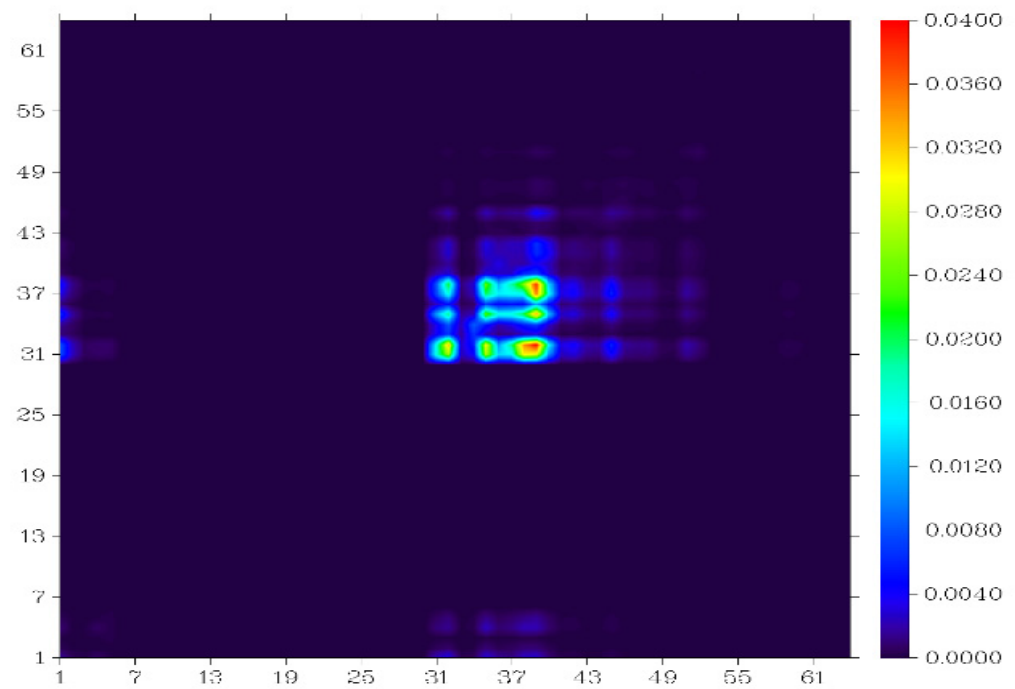
O4



O5



O6



O7

Figure S6: Electron-hole overlap transition density matrix of each non-hydrogen atom within each compound

Table S8: Cartesian coordinates of **O1**

C	8.956100	-0.668900	-3.066000
O	9.598000	-0.693100	-1.780400
C	10.834500	-0.080400	-2.125900
C	11.901800	0.419700	-1.093700
C	12.955800	1.214600	-1.421400
S	11.917800	0.045800	0.640100
C	13.918700	1.481300	-0.230100
H	13.126100	1.599600	-2.402900
C	13.496100	0.838800	0.903800
H	14.821200	2.066900	-0.287400
C	14.229200	0.805600	2.239300
H	14.941500	1.569400	2.523300
C	13.943900	-0.228600	3.132400
C	13.222500	-1.531900	2.566700
N	12.690600	-2.492700	2.149700
C	14.264800	0.035500	4.609800
O	14.896700	1.102900	4.986600
O	13.777500	-0.855400	5.624400
H	13.282500	-0.325500	6.275700
N	9.783100	-0.379800	-4.019800
N	10.970200	0.042300	-3.413400
C	7.466600	-0.959400	-3.309600
O	6.531600	-1.245400	-2.265100
C	5.324100	-1.062800	-3.010300
N	6.915300	-0.963200	-4.477000
N	5.535900	-1.023000	-4.286200
C	3.933600	-0.915800	-2.369200
C	3.793600	-0.975600	-0.976100
C	2.806500	-0.728900	-3.179300
C	2.525600	-0.846000	-0.393100
H	4.654600	-1.117400	-0.357000
C	1.538100	-0.596200	-2.596200
H	2.914400	-0.684800	-4.243200

C	1.396600	-0.658800	-1.201700
H	2.418400	-0.895200	0.670000
H	0.677500	-0.454400	-3.216200
C	0.004100	-0.509700	-0.555200
C	-0.142400	-0.617400	0.835800
C	-1.117700	-0.273800	-1.358800
C	-1.415800	-0.506400	1.421900
H	0.718000	-0.780400	1.451000
C	-2.380600	-0.113500	-0.771900
H	-1.010200	-0.211500	-2.421300
C	-2.538300	-0.250000	0.616200
H	-1.527800	-0.614400	2.480900
H	-3.230200	0.099100	-1.386000
N	-3.888200	-0.122900	1.204300
C	-4.698900	-1.299400	0.827000
C	-4.637200	-2.484900	1.581200
C	-5.542300	-1.229700	-0.289900
C	-5.441800	-3.584700	1.231600
H	-3.982600	-2.549500	2.424900
C	-6.358600	-2.318500	-0.623800
H	-5.570700	-0.340200	-0.883400
C	-6.299600	-3.503000	0.123100
H	-5.396300	-4.486400	1.805000
H	-7.023000	-2.250400	-1.459400
C	-4.528500	1.113400	0.709800
C	-4.905600	1.254800	-0.634900
C	-4.751700	2.169200	1.612500
C	-5.499500	2.451600	-1.067700
H	-4.736200	0.459400	-1.330900
C	-5.354100	3.360800	1.179900
H	-4.472200	2.059100	2.639800
C	-5.714100	3.509600	-0.164700
H	-5.776500	2.568800	-2.095200
H	-5.537500	4.153600	1.876000

C	-8.483100	-4.241800	-0.780500
C	-7.489900	-5.520300	0.880900
C	-8.757300	-3.510500	-1.876000
C	-9.494900	-4.723700	0.024700
C	-6.641200	-6.161400	1.704400
C	-8.852600	-5.558800	1.094300
C	-10.108300	-3.211700	-2.154000
H	-7.972200	-3.163700	-2.514700
C	-10.799200	-4.476700	-0.186000
C	-7.185100	-6.898900	2.776400
H	-5.585100	-6.109500	1.548800
C	-9.433100	-6.243300	2.093900
C	-11.134400	-3.697100	-1.305200
H	-10.357500	-2.615000	-3.005300
H	-11.552800	-4.861900	0.472400
C	-8.588500	-6.944800	2.968900
H	-6.536800	-7.423000	3.445000
H	-10.498300	-6.255900	2.216100
H	-12.160100	-3.474500	-1.516100
H	-9.002900	-7.508300	3.778200
C	-5.636100	5.982000	-0.153400
C	-7.709000	4.939900	-0.153900
C	-4.372100	6.357200	-0.410900
C	-6.463800	6.746600	0.630200
C	-8.768000	4.120400	-0.314800
C	-7.808500	6.078700	0.628900
C	-3.899000	7.544500	0.178700
H	-3.744200	5.766200	-1.045400
C	-6.075000	7.888400	1.228500
C	-9.979300	4.469300	0.326800
H	-8.691000	3.231600	-0.902900
C	-8.930000	6.466100	1.251000
C	-4.753000	8.315700	1.004300
H	-2.893200	7.860400	0.003500

H	-6.744900	8.450300	1.847800
C	-10.060400	5.651600	1.105400
H	-10.837500	3.840300	0.224900
H	-8.959500	7.365700	1.833400
H	-4.396000	9.220700	1.452600
H	-10.977300	5.920300	1.584600
N	-7.135700	-4.650900	-0.281400
N	-6.310900	4.761000	-0.667300

Table S9: Cartesian coordinates of **O2**

C	6.927500	-0.922600	-0.178900
C	5.825500	-1.777900	-0.045700
C	4.582800	-1.261900	0.115300
C	4.399700	0.127100	0.148600
C	5.501800	0.982500	0.015400
C	6.744500	0.466400	-0.145600
H	5.965200	-2.838500	-0.071100
H	3.741300	-1.915000	0.217000
H	5.362000	2.043000	0.040800
H	7.585900	1.119500	-0.247400
O	8.238800	-1.467100	-0.348800
H	8.772200	-0.860900	-0.868100
C	2.987500	0.713500	0.331600
O	1.804400	-0.080700	0.472200
C	0.829400	0.944100	0.249900
C	-0.523200	0.692400	-0.016400
C	-1.466000	1.654800	-0.230900
S	-1.247500	-0.912900	-0.114300
C	-2.793100	1.143700	-0.304900
H	-1.232200	2.694900	-0.322800
C	-2.864700	-0.209500	-0.146900
H	-3.652300	1.762700	-0.457700
C	-4.173500	-1.009500	-0.010000
H	-4.140700	-2.071900	0.113300

C	-5.366700	-0.368100	-0.045700
C	-5.413900	1.161000	-0.223200
N	-5.449000	2.299400	-0.355300
C	-6.675400	-1.168100	0.091200
O	-6.636900	-2.417500	0.236200
O	-7.821200	-0.552100	0.056900
H	-8.637000	-1.050800	0.142200
N	2.731700	1.980200	0.370200
N	1.343100	2.128600	0.317700

Table S10: Cartesian coordinates of **O3**

C	6.019500	-1.242800	0.301900
C	4.855500	-1.785800	-0.262900
C	3.700300	-0.998400	-0.375600
C	3.708700	0.329000	0.073500
C	4.867400	0.865800	0.648500
C	6.022200	0.083800	0.759700
H	4.850600	-2.799600	-0.607100
H	2.812200	-1.410000	-0.804200
H	4.868300	1.874300	1.001600
H	6.907100	0.500200	1.195000
O	7.199700	-2.040300	0.412300
C	2.450700	1.206100	-0.062300
O	1.215800	0.764800	-0.652000
C	0.364800	1.838000	-0.216300
C	-1.171500	1.804800	-0.289900
C	-1.980400	2.822000	0.103600
S	-2.133500	0.442800	-0.891300
C	-3.479700	2.425600	0.068400
H	-1.624700	3.780800	0.411900
C	-3.663900	1.141900	-0.339600
H	-4.275000	3.081000	0.343700
C	-5.014400	0.402100	-0.319200
H	-5.518200	0.552600	-1.251300

H	-5.618700	0.783400	0.477700
C	-4.771600	-1.101500	-0.106300
H	-4.169600	-1.481400	-0.906000
C	-4.041500	-1.316000	1.234900
N	-3.500100	-1.474900	2.229300
C	-6.120800	-1.846300	-0.081400
O	-7.156600	-1.262900	0.333700
O	-6.195700	-3.201800	-0.531400
H	-7.066900	-3.369900	-0.898000
N	2.372400	2.431400	0.344700
N	1.047700	2.832500	0.249100
C	7.995300	-1.897000	-0.767200
H	8.877600	-2.495300	-0.675600
H	7.432700	-2.219600	-1.618800
H	8.271300	-0.870800	-0.890800

Table S11: Cartesian coordinates of **O4**

C	-6.387700	-1.486200	-0.183700
C	-5.133700	-2.101300	-0.072500
C	-3.984800	-1.321400	0.104600
C	-4.089200	0.073900	0.168000
C	-5.345100	0.688400	0.067400
C	-6.494000	-0.092000	-0.109600
H	-5.053400	-3.166200	-0.123500
H	-3.027900	-1.791100	0.190900
H	-5.426900	1.753300	0.124800
H	-7.452300	0.376400	-0.188700
C	-2.823000	0.931400	0.346600
O	-1.500200	0.392200	0.446700
C	-0.760300	1.600200	0.230700
C	0.742700	1.642200	-0.100400
C	1.458400	2.781300	-0.306300
S	1.781800	0.217000	-0.258800
C	2.980100	2.502100	-0.417100

H	1.024300	3.757500	-0.371800
C	3.268100	1.180700	-0.282300
H	3.717600	3.261800	-0.569200
C	4.689300	0.603700	-0.158500
H	5.536800	1.256400	-0.171700
C	4.864300	-0.732800	-0.030700
C	3.640100	-1.668500	-0.023700
N	2.717200	-2.362800	-0.019400
C	6.288400	-1.309300	0.108700
O	7.283800	-0.537300	0.117100
O	6.480300	-2.719500	0.228800
H	7.271000	-2.891400	0.746600
N	-2.829800	2.222300	0.415900
N	-1.502100	2.652900	0.340700
N	-7.592000	-2.303200	-0.379000
H	-7.976900	-2.548500	0.509100
H	-8.267500	-1.782200	-0.901700

Table S12: Cartesian coordinates of **O5**

C	-4.675400	-3.095900	-0.219300
O	-5.347200	-1.836800	-0.306800
C	-6.574000	-2.202400	0.340400
C	-7.643100	-1.193100	0.803900
C	-8.754300	-1.514700	1.502600
S	-7.599000	0.557000	0.488000
C	-9.713300	-0.296200	1.669600
H	-8.967900	-2.497000	1.877200
C	-9.274200	0.794600	1.033500
H	-10.623100	-0.335000	2.204900
C	-10.123900	2.059600	0.832600
H	-10.905400	2.326500	1.529100
C	-9.925900	2.849700	-0.263600
C	-9.373800	2.152900	-1.587000
N	-8.965200	1.637200	-2.566500

C	-10.269500	4.364400	-0.160300
O	-11.166500	4.783500	0.644900
O	-9.589200	5.363800	-0.950300
H	-9.547600	6.184000	-0.413800
N	-5.475300	-4.059200	0.100200
N	-6.683900	-3.484100	0.484800
C	-3.172200	-3.286100	-0.471800
O	-2.279000	-2.225700	-0.827700
C	-1.040400	-2.898600	-0.578300
N	-2.568400	-4.423600	-0.376500
N	-1.196400	-4.174500	-0.442200
C	0.319900	-2.186800	-0.477200
C	0.397300	-0.797700	-0.640000
C	1.480400	-2.929400	-0.222700
C	1.636000	-0.150500	-0.549200
H	-0.489400	-0.231100	-0.833400
C	2.719300	-2.281900	-0.130600
H	1.420300	-3.990600	-0.098400
C	2.796200	-0.892000	-0.294000
H	1.696300	0.910200	-0.674900
H	3.606100	-2.848600	0.063200
C	4.155000	-0.177200	-0.191700
C	4.234000	1.210100	-0.378800
C	5.311400	-0.912800	0.088300
C	5.474200	1.862500	-0.300600
H	3.346400	1.771600	-0.581000
C	6.544500	-0.258200	0.200600
H	5.253500	-1.974600	0.215400
C	6.629600	1.129300	-0.004100
H	5.535400	2.917900	-0.459900
H	7.425900	-0.819900	0.432000
N	7.944300	1.786800	0.088900
C	8.777800	1.355800	-1.039300
C	8.695500	2.013200	-2.272600

C	9.667500	0.286700	-0.870500
C	9.513300	1.607100	-3.335800
H	8.010500	2.824600	-2.402400
C	10.489800	-0.114600	-1.930000
H	9.722200	-0.219900	0.070900
C	10.412500	0.545200	-3.163500
H	9.451500	2.107600	-4.279100
H	11.177000	-0.924100	-1.797100
H	11.040300	0.238700	-3.973500
C	8.583000	1.413400	1.353700
C	8.940100	0.086100	1.610600
C	8.829500	2.407700	2.309800
C	9.530000	-0.249900	2.836900
H	8.752500	-0.671000	0.878500
C	9.454700	2.079500	3.517000
H	8.548700	3.421700	2.111100
C	9.797100	0.748500	3.785300
H	9.775000	-1.268700	3.050200
H	9.671500	2.844900	4.233100
H	10.262400	0.493900	4.714000

Table S13: Cartesian coordinates of **O6**

C	-0.750500	1.743200	0.464700
O	0.523600	1.563100	0.588700
C	0.708800	1.104200	1.791300
N	-1.394800	1.391200	1.600800
N	-0.456300	1.004900	2.459800
C	2.041700	0.696800	2.228500
C	2.996900	0.572700	1.217400
C	2.395100	0.421700	3.554300
C	4.286400	0.195300	1.501400
H	2.750300	0.755600	0.176600
C	3.717500	0.053000	3.852700
H	1.667400	0.512400	4.355000

C	4.696300	-0.061700	2.823300
H	4.927700	0.117300	0.641800
H	3.945500	-0.120100	4.894000
C	6.128600	-0.424800	3.095500
C	7.109800	-0.361200	2.067200
C	6.553600	-0.821400	4.382600
C	8.439600	-0.660600	2.319100
H	6.904000	-0.067800	1.053400
C	7.886300	-1.140900	4.621500
H	5.882100	-0.895100	5.222700
C	8.829800	-1.051800	3.591000
H	9.166400	-0.596600	1.516100
H	8.192400	-1.437500	5.618200
N	10.187400	-1.343700	3.838700
C	10.461800	-2.630100	4.393400
C	10.080100	-3.777800	3.688100
C	11.109800	-2.779400	5.626900
C	10.379800	-5.047200	4.185800
H	9.587800	-3.688400	2.724600
C	11.377800	-4.041400	6.136500
H	11.403100	-1.927400	6.223500
C	11.045700	-5.212900	5.425700
H	10.111700	-5.873400	3.552300
H	11.846100	-4.047000	7.092700
C	11.021900	-0.255600	4.207800
C	10.806100	0.453400	5.399400
C	12.118000	0.060800	3.401300
C	11.723300	1.419200	5.811500
H	9.962400	0.216600	6.034200
C	13.012900	1.054000	3.792700
H	12.292000	-0.482400	2.480700
C	12.844300	1.717400	5.019200
H	11.559000	1.923400	6.752500
H	13.873900	1.250700	3.168800

C	-1.347900	2.191700	-0.810700
C	-0.636700	2.904400	-1.719300
H	-1.104100	3.228200	-2.643300
C	0.726000	3.350600	-1.509900
N	1.814900	3.709800	-1.347800
C	-2.751900	1.867500	-1.084900
O	-3.556800	1.328300	-0.206700
C	-4.729800	1.339900	-0.780400
N	-3.403200	2.186900	-2.218900
N	-4.667200	1.869400	-2.017100
C	-5.955700	1.231600	-0.006500
C	-5.959700	0.673900	1.285200
C	-7.085800	1.880100	-0.501200
C	-7.076500	0.840000	2.109100
H	-5.082000	0.173100	1.679200
C	-8.166800	2.082400	0.324500
H	-7.106100	2.325800	-1.489000
C	-8.156800	1.609700	1.648900
H	-7.046900	0.463200	3.125200
H	-8.997900	2.655900	-0.069500
C	-9.246700	2.028900	2.538700
C	-9.792200	1.201400	3.528100
C	-9.733900	3.338200	2.383600
C	-10.876700	1.660600	4.280500
H	-9.427100	0.192100	3.675500
C	-10.775100	3.804000	3.150200
H	-9.310600	4.020700	1.658000
C	-11.388000	2.963400	4.080900
H	-11.340800	0.993100	4.996700
H	-11.135900	4.804300	2.955800
N	-12.594400	3.380900	4.715800
C	-12.904500	4.781900	4.839900
C	-11.976400	5.716600	5.337100
C	-14.158900	5.250100	4.412600

C	-12.318300	7.079700	5.418100
H	-10.996700	5.389600	5.669600
C	-14.484400	6.584300	4.473600
H	-14.907100	4.585400	4.001800
C	-13.582600	7.533200	4.972700
H	-11.577500	7.756900	5.803800
H	-15.476600	6.849400	4.145500
C	-13.700800	2.475300	4.691200
C	-13.847900	1.524800	3.650200
C	-14.717600	2.617200	5.648900
C	-14.996600	0.752300	3.570100
H	-13.109500	1.403400	2.859100
C	-15.861900	1.848100	5.563300
H	-14.631900	3.346500	6.454500
C	-16.019200	0.910900	4.521700
H	-15.086900	0.075400	2.730800
H	-16.612300	1.992300	6.332200
C	-13.742900	9.836800	6.082600
C	-15.016400	9.486000	4.222500
C	-12.783900	9.708300	7.232500
C	-14.702400	10.939900	6.004100
C	-15.524600	8.980600	2.899300
C	-15.514400	10.708600	4.819100
C	-12.809000	10.964900	8.117300
H	-11.743400	9.623200	6.861900
C	-14.915700	11.933400	7.102700
C	-16.446200	10.009000	2.226800
H	-14.674000	8.779700	2.211000
C	-16.716900	11.444900	4.307200
C	-14.238500	11.438800	8.390600
H	-12.267800	10.748600	9.062200
H	-16.000500	12.036100	7.322600
C	-17.435500	10.609900	3.229500
H	-16.975600	9.515000	1.384700

H	-17.447100	11.606700	5.128500
H	-14.251900	12.252300	9.145300
H	-18.199800	11.235200	2.720800
C	-18.468000	0.521300	4.943900
C	-17.260700	-1.259000	4.179100
C	-18.909300	1.917300	5.273500
C	-19.325400	-0.636600	5.090700
C	-16.092400	-2.159500	3.880200
C	-18.573000	-1.780400	4.563600
C	-20.420900	1.960300	5.514800
H	-18.674000	2.604400	4.431400
C	-20.659000	-0.568300	5.773400
C	-16.502600	-3.630700	3.849800
H	-15.613100	-1.929200	2.910800
C	-18.800700	-3.243000	4.802500
C	-20.861400	0.814600	6.431000
H	-20.681800	2.950500	5.945200
H	-20.715600	-1.324000	6.584300
C	-17.452100	-3.957500	5.005300
H	-15.578700	-4.245700	3.894600
H	-19.436000	-3.401800	5.699400
H	-21.921400	0.933500	6.735700
H	-17.615000	-5.051600	5.071600
C	14.654600	3.456000	4.683100
C	14.489300	2.502400	6.748800
C	14.374600	3.903500	3.279800
C	15.842700	3.858700	5.416300
C	14.188300	1.482800	7.815400
C	15.726600	3.282000	6.753600
C	15.318200	5.054400	2.895200
H	13.335200	4.288800	3.203600
C	16.965800	4.631400	4.796000
C	15.208400	1.533300	8.960000
H	13.177200	1.616600	8.245600

C	16.806000	3.065300	7.772200
C	16.770200	4.740000	3.271800
H	15.219200	5.256600	1.808000
H	17.935500	4.118800	4.968500
C	16.637700	1.687100	8.430500
H	15.102800	0.611300	9.570500
H	17.814500	3.137500	7.312000
H	17.462600	5.508900	2.869900
H	17.367500	1.584400	9.260200
C	12.504600	-6.835500	6.798600
C	10.942300	-7.778300	5.423000
C	13.435100	-5.897200	7.530300
C	12.766700	-8.271600	6.787000
C	9.741100	-8.047700	4.558300
C	11.790200	-8.862400	5.892200
C	14.541200	-6.631500	8.294500
H	12.891700	-5.331500	8.312000
C	14.018800	-8.884800	7.337800
C	9.441300	-9.551900	4.460700
H	8.840800	-7.553600	4.981700
C	11.672300	-10.278700	5.419600
C	15.098700	-7.806400	7.497400
H	15.335000	-5.899900	8.556700
H	14.406500	-9.667900	6.653900
C	10.716100	-10.361200	4.219100
H	8.703500	-9.719400	3.647800
H	12.659200	-10.654300	5.077200
H	15.977000	-8.239100	8.019100
H	10.481800	-11.425700	4.008900
N	11.423300	-6.522900	5.906900
N	13.852500	2.608600	5.483100
N	-14.009600	8.901100	5.043400
N	-17.200700	0.127100	4.462000

Table S14: Cartesian coordinates of O7

C	0.291400	1.559200	0.378800
O	1.535300	1.776300	-0.255600
C	2.122600	0.603800	0.176100
N	0.058100	0.339300	0.681100
N	1.272000	-0.270700	0.592900
C	3.631000	0.428500	0.141400
C	4.397500	1.508600	-0.283800
C	4.256000	-0.780900	0.508500
C	5.790500	1.418600	-0.346300
H	3.902600	2.399200	-0.557300
C	5.656400	-0.876500	0.446600
H	3.680300	-1.633300	0.833800
C	6.419900	0.220600	0.016600
H	6.363600	2.262000	-0.675300
H	6.141700	-1.787600	0.720100
C	7.947500	0.114000	-0.052000
C	8.714600	1.196700	-0.508700
C	8.571900	-1.072700	0.339800
C	10.112000	1.083700	-0.583600
H	8.235700	2.109400	-0.794000
C	9.967600	-1.172200	0.301500
H	7.983200	-1.903800	0.673400
C	10.739500	-0.100000	-0.173700
H	10.696400	1.901300	-0.948100
H	10.446200	-2.073700	0.623300
N	12.203900	-0.247300	-0.236400
C	12.543100	-1.218900	-1.283700
C	12.669300	-0.809900	-2.617000
C	12.751100	-2.560600	-0.937600
C	13.017600	-1.742400	-3.603500
H	12.501400	0.213100	-2.881600
C	13.107100	-3.491300	-1.921000
H	12.643000	-2.872400	0.080100

C	13.240000	-3.082200	-3.254600
H	13.113900	-1.432000	-4.623100
H	13.277900	-4.513700	-1.653800
H	13.512200	-3.792600	-4.006300
C	12.699800	-0.716300	1.060300
C	12.346300	-1.978100	1.549900
C	13.534100	0.122600	1.810400
C	12.814000	-2.392700	2.804900
H	11.712800	-2.618900	0.973800
C	14.037000	-0.308300	3.042300
H	13.795600	1.090300	1.434700
C	13.668400	-1.562100	3.545400
H	12.517300	-3.341900	3.199300
H	14.702400	0.319500	3.598400
H	14.039300	-1.886300	4.494600
C	-0.631100	2.770100	0.624200
C	-0.591000	3.625500	1.600000
H	-1.490500	3.855000	2.115000
C	0.733200	4.280800	1.886700
N	1.661400	4.740100	2.087700
C	-1.534700	3.291500	-0.464500
O	-1.966600	2.640200	-1.660700
C	-3.225500	3.268600	-1.436200
N	-2.000700	4.494500	-0.349600
N	-3.207400	4.496500	-1.059300
C	-4.444600	2.490700	-1.463400
C	-4.542700	1.321700	-2.175900
C	-5.414400	2.982600	-0.624700
C	-5.647600	0.533200	-1.937800
H	-3.773700	1.038000	-2.872300
C	-6.494200	2.194500	-0.347200
H	-5.288200	3.948200	-0.185000
C	-6.598600	0.955500	-0.995100
H	-5.749100	-0.390200	-2.454900

H	-7.223100	2.515000	0.366400
C	-7.782000	0.074700	-0.659700
C	-7.920800	-1.156200	-1.283700
C	-8.700100	0.498500	0.313300
C	-9.015400	-1.960500	-0.980200
H	-7.186600	-1.480000	-2.005600
C	-9.804400	-0.302100	0.611200
H	-8.556300	1.435200	0.819600
C	-9.952400	-1.535700	-0.032900
H	-9.138700	-2.906100	-1.477900
H	-10.528800	0.024000	1.328100
N	-11.106200	-2.391600	0.250800
C	-11.641100	-2.056300	1.579500
C	-11.150000	-2.692800	2.726000
C	-12.641700	-1.080700	1.692800
C	-11.654900	-2.344100	3.988800
H	-10.384500	-3.445700	2.642200
C	-13.144700	-0.735600	2.953800
H	-13.021200	-0.595700	0.810900
C	-12.651800	-1.365100	4.101500
H	-11.278100	-2.825900	4.871400
H	-13.910000	0.014300	3.038100
H	-13.038800	-1.098100	5.067600
C	-12.160700	-2.171100	-0.760900
C	-12.552000	-0.873700	-1.100800
C	-12.760700	-3.275300	-1.378900
C	-13.554800	-0.679100	-2.056700
H	-12.087400	-0.029400	-0.622700
C	-13.741400	-3.078800	-2.355900
H	-12.460600	-4.276200	-1.108600
C	-14.143800	-1.779700	-2.691900
H	-13.872800	0.316600	-2.304800
H	-14.184300	-3.922300	-2.852100
H	-14.903800	-1.627800	-3.438100

References

- 1 J. Preat, D. Jacquemin, C. Michaux, and E.A. Perpète, *Chem. Phys.*, 2010, **376**, 1-3, 56-68
- 2 Y. Kurumisawa, T. Higashino, S. Nimura, Y. Tsuji, H. Liyama, and H. Imahori, *J. Am. Chem. Soc.*, 2019, **141**, 25,
- 3 S. Arrechea, J.N. Clifford, L. Pelleja, A. Aljarilla, P. de la Cruz, E. Palomares, and F. Langa, 2016, **126**, 147-153
- 4 R. Samae, P. Surawatanawong, U. Eiamprasert, S. Pramjit, L. Saengdee, P. Tangboriboonrat, and S. Kiatisevi, *Eur. J. Chem.*, 2016, **21**, 3536-3549
- 5 W. Sharmoukh, J. Cong, B.A. Ali, N.K. Alam, and L. Kloo, *Am. Chem. Soc.*, 2020, **5**, 27, 16856-16864
- 6 P. Gao, H.N. Tsao, M. Grätzel, and M.K. Nazeeruddin, *Org. Lett.*, 2012, **14**, 17, 4330-4333
- 7 Y. Mu, H. Wu, G. Dong, Z. Shen, S. Li, and M. Zhang, *J. Mater. Chem. A*, 2018, **6**, 21493-21500
- 8 Z. Wu, X. Li, H. Agren, J. Hua, and H. Tian, *Appl. Mater. Interfac.*, 2015, **7**, 48, 26355-26359
- 9 L. Zhang, J.M. Cole, P.G. Waddell, K.S. Low, and X. Liu, *Sus. En. Eng.*, **1**, 11, 1440-1452
- 10 B. Cecconi, A. Mordini, G. Reginato, L. Zani, M. Taddei, F.F. de Biani, F. De Angelis, G. Marotta, P. Salvatori, and M. Calamante, *As. J. Org. Chem.*, **3**, 2, 140-152
- 11 P. Ganesan, A. Chandiran, P. Gao, R. Rajalingam, M. Grätzel, and M.K. Nazeeruddin, *J. Phys. Chem. C*, 2014, **118**, 30, 16896-16903
- 12 N. Kungwan, P. Khongpracha, S. Namuangruk, J. Meeprasert, C. Chitpakalee, and S. Jungsuttiwong, *Theor. Chem. Acc.*, 2014, **133**, 1523
- 13 P. Naik, M.R. Elmorsy, R. Su, D.D. Babu, A. El-Shafei, A.V. Adhikari, *Sol. En.*, 2017, **153**, 600-610
- 14 X. Zarate, S. Schott-Verdugo, A. Rodrigues-Serrano, and E. Schott, *J. Phy. Chem. A*, 2016, **120**, 1613-1624
- 15 U. Mubashar, A. Farhat, R.A. Khera, N. Iqbal, R. Saleem, and J. Iqbal, *J. Mol. Mod.*, 2021, **27**, 216, 1-13
- 16 Y. Mu, H. Wu, G. Dong, Z. Shen, S. Li, and M. Zhang, *J. Mater. Chem. A*, 2018, **6**, 21493-21500
- 17 D. Ompang, and J. Singh, *Chem. Phys. Chem.*, 2015, **16**, 1281-1285
- 18 A. Pivrikas, G. Juška, R. Österbacka, M. Westerling, M. Viliūnas, K. Arlauskas, and H. Stubb, *Phys. Rev. B*, 2005, **71**, 1-5